Loughborough
University

This item was submitted to Loughborough University as an MPhil thesis by the author and is made available in the Institutional Repository (https://dspace.lboro.ac.uk/) under the following Creative Commons Licence conditions.

For the full text of this licence, please go to:
http://creativecommons.org/licenses/by-nc-nd/2.5/

Numerical Solution of the Non-Linear Schroedinger Equation :
The Half-Line Problem
and
Dynamical Systems and Bifurcations of Vector Fields

by
Maria S. Zakynthinaki

A Master's Thesis

Submitted in partial fulfilment of the requirements
for the award of

Master of Philosophy of the Loughborough University of Technology

25 March 1997

Acknowledgements

I would like to thank Prof A.S.Fokas (Imperial College of Science, Technology and Medicine) for his support, as well as his considerable recommendations, concerning the first part of my thesis.

Thanks are due to Dr G.Gaeta (Loughborough University) for his guidance, during the second part of my work. Without his tireless suggestions this thesis would not have been possible.

I would also like to express my indebtedness to Prof Y.G.Saridakis (Technical University of Crete) for his helpful comments.

My deepest gratitude, however, is to my family and friends in England and Greece, who have been for me the source of motivation, encouragement and inspiration.

Abstract

Solutions to the nonlinear Schrödinger equation with potential $V(u) = -\lambda u |u|^2$ have been theoretically and numerically calculated, revealing the formation of solitons. In this study the finite element method with linear basis functions, distinguished for its simplicity and effective applicability, is considered and a predictor-corrector scheme is applied to simulate the propagation in time. Numerical experiments include the propagation of a single soliton form, a two-soliton collision, as well as the formation of more than one solitons from non-soliton initial data. The important problem of boundary reflections has been successfully overcome by the implementation of absorbing boundaries, a method that in practice achieves a gradual reduction of the wave amplitude at the end of each time step.

The second part of this work deals with dynamical systems of the form $\dot{\vec{x}} = \vec{V}(\mu, \vec{x}), \vec{x} \in \mathcal{R}^n$. The dynamics of such systems near their equilibrium point depends strongly on the adjustable parameter μ, as it is possible for the system to lose its hyperbolicity and a bifurcation to occur. After reviewing aspects of linearisation, the prospect of change in the equilibrium solutions has been studied, both for flows and maps, in terms of the eigenvalues of the linearised system. In the study of steady-state bifurcation, elements of saddle-node, transcritical, pitchfork, as well as period-doubling bifurcation are considered. Finally, the case when equilibrium solutions persist, known as Hopf bifurcation, has also been included.

TABLE OF CONTENTS

PART TWO: DYNAMICAL SYSTEMS AND BIFURCATIONS
OF VECTOR FIELDS

PART ONE

Numerical Solution of the

Non-Linear Schrödinger Equation :

The Half-Line Problem

I. INTRODUCTION

Ia. Solitons - A review

The first observation of a soliton was made by J. Scott Russel [29] in 1834. He was looking at a boat moving on a shallow canal and noticed that, when the boat suddenly stopped, the wave that was pushing at its prow took its own life : "it accumulated round the prow of the vessel in a state of violent agitation, then suddenly, leaving it behind, rolled forward with great velocity, assuming the form of a large solitary elevation, a rounded, smooth and well defined heap of water which continued its course along the channel apparently without change of form or diminution of speed". J. Scott Russel followed the wave along the canal for several Kms. He was so impressed by his "great solitary wave", as he called it, that he spent ten years of his life to study experimentally the properties of this singular and beautiful phenomenon.

The analytical explanation of Scott Russel's observations was provided only much later. D. Korteweg and G. de Vries in 1895 [4, 21] provided an extended study of the non-linear wave propagation, which led to the formation of one of the most well known and important equations in the field of non-linear physics, the *KdV* equation. The phenomenon was then forgotten until 1965 when N. Zabusky and M. Kruskal [34] coined the word *soliton* to describe this solitary wave which proved to have particle-like properties. They also provided a fundamental understanding of the origin of the soliton and initiated the development of mathematical methods, which started a soliton industry in applied mathematics.

Whatever the actual experiment made, solitons are always impressive to the observer: their properties are against our intuition, built on observation of small amplitude linear waves that spread over as they propagate. Solitons are extremely robust.

The special properties of these solitary waves are, in brief, the following [9, 32]

- they propagate at constant speed without changing their shape

- they are extremely stable to perturbations and in particular to collisions with small amplitude linear waves

- they are stable even with respect to collisions with other solitons.

The world of solitons includes various types of localised non-linear excitations. Although they may look different, they have in common their exceptional stability and their particle-like properties which distinguish them from the linear waves that we are used to consider. In fact, linear systems do not carry exact soliton solutions in the strict mathematical sense (which implies an infinite life-time and an infinity of conservation laws) but *quasi-solitons*, which have most of the features of true solitons. This is why physicists often use the word soliton in a loose way, which does not always agree with mathematical rigour. Some of those quasi-solitons can be observed by satellites as they propagate over hundreds of kilometers in a shallow sea, providing impressive illustrations of the soliton concepts, and also of their power.

Ib. The non-linear Schrödinger equation

The basis of the mathematical formalism of quantum mechanics lies in the fact that any state of the system can be described at a given moment by the generally complex *wavefunction* of the system $u(x, t)$. The evolution of the system is described by the Schrödinger equation which, in its general form, is given by the relation [24]

$$i\frac{\partial u}{\partial t} = \hat{H}u \qquad , \qquad (1)$$

where $\hat{H}$ is the Hamiltonian of the system,

$$\hat{H} \equiv -\left(\frac{\hbar^2\nabla^2}{2m}\right) + \hat{V} \qquad .$$

In the above relation, $\hat{V}$ corresponds to the potential describing the system, m denotes the mass of the particle under study and $\hbar$ is the well known Planck constant. In the present study the Hamiltonian of the system is expressed in the form

$$\hat{H} \equiv -\nabla^2 + \hat{V} \qquad ,$$

where it is assumed that $\hbar^2/2m = 1$ for normalisation purposes.

If now $u(x, t)$ is a complex field governing the evolution of any weakly non-linear, strongly dispersive and almost monochromatic wave, the Hamiltonian of the system is given by the expression

$$\hat{H}u = -\frac{\partial^2 u}{\partial^2 x} - \lambda u|\, u\,|^2,$$

so the Schrödinger equation becomes

$$i\frac{\partial u}{\partial t} + \frac{\partial^2 u}{\partial^2 x} + \lambda u|\, u\,|^2 = 0. \qquad (2)$$

Many theoretical, numerical, as well as experimental investigations have confirmed the validity of the above equation, known in the mathematical community with the short name *NLS*, for a variety of problems. The pure initial value problem was solved exactly by V. Zakharov and D. Shabat in 1972 [33] using the inverse scattering method (see also

4

M. Ablowitz [1]), provided the initial condition $u(x, 0)$ vanishes for sufficiently large $\mid x \mid$. Since then, much theoretical work has been done by A. Fokas, I. Gelfand, V. Zakharov and A. Its [10, 11, 12] on the problem of the inverse scattering transform and the linearisation of the initial boundary problem of the NLS. They found analytical expressions for the soliton solutions, both in the one- and in the two-dimensional case.

Apart from its physical significance, the NLS is of considerable interest to the numerical analyst in its own right. Some of its most attractive features are, in review,

- non-linearity and dispersion, which under favourable conditions allow soliton solutions [33],

- instability and recurrence [23] and

- bound states of two or more solitons [19].

Among the earlier methods used for solving the NLS numerically are the *Fourier* and *split-step* methods, as well as the methods employed by B. Lake et al. [23] and R. Hardin and F. Tappert [18]. Other referred authors used mainly finite difference or finite element methods to discretise the space variable (see also [16, 31]). For the discretisation of the time variable, J. Sanz-Serna [26, 27, 28] used an explicit, variable time step leapfrog scheme, M. Delfour et al. [8] a modified Crank-Nicolson scheme, D. Griffiths et al. [15] a predictor-corrector method and B. Herbst et al. [19] the midpoint rule.

Ic. The numerical method

The subject of numerical analysis is concerned with devising methods for approximating, in an efficient manner, the solutions to mathematically expressed problems. The efficiency of the method depends both upon the accuracy required, and the ease with which it can be implemented. In the NLS case, as in dealing with every other mathematical problem based on a physical phenomenon, it is rather more appropriate to find an approximate solution to the more complicated mathematical model, than to find an exact solution of a simplified model [5].

Numerical analysts are also concerned with the concept of eliminating the so-called round off error, i.e. the unavoidable errors which can be accumulated during the numerical procedure. To reduce the effects of rounding errors, and thus ensure the algorithm's stability, usually large-order digit arithmetic is being used, such as the double precision (real*8) arithmetic. In the case of a large number of subsequent computations, the serious growth of rounding off error can be said not to be eliminated entirely, though sufficiently postponed.

If $\Psi(x,t)$ is a solution to the given problem, numerically obtained, then it will not be given as a continuous function of x and t; instead, it will be generated at the various *mesh points* in the interval $[x_L, x_R]$, in which the solution is to be found. In the present study it is assumed that the mesh points are equally distributed throughout $[x_L, x_R]$. This condition can be ensured by choosing an integer N, and selecting the points $\{x_1, x_2, \cdots, x_N\}$ such that

$$x_i = x_1 + ih, \qquad for \quad i = 1, 2, \cdots, N \quad .$$

The common distance between the points is the chosen step size $h = (x_N - x_1)/N$.

Letting now $\Psi^{(0)}(x)$ be the initial condition to the problem under consideration, and choosing an appropriate time step τ, the numerical procedure finds a solution for every given time $t = k\tau$, where k is an integer. In other words, the outcome of the numerical procedure is in fact a sequence of solutions $\{\Psi^{(k)}(x)\}$, and the chosen numerical method is considered satisfactory for the problem if this sequence satisfactory approximates the exact solution $\tilde{\Psi}(x,t)$.

Id. The method of absorbing boundaries

In the numerical simulation of the wave propagation implemented in the present study and also in the referred numerical simulation experiments, there is always the need to eliminate spurious events generated by the boundaries of the numerical grid. These events take place because only a finite region of space is covered by the numerical mesh, and appear in the form of reflections from the boundaries. R. Kosloff and D. Kosloff in their study in [22] presented a systematic method of eliminating the boundary reflections through the application of *absorbing* boundaries. The scheme is based on a simple modification of the wave equation, so that the wave amplitude becomes attenuated at the boundary region of the grid.

In practice the method of absorbing boundaries achieves a gradual reduction of the wave amplitude at the end of each time step. This reduction should take place in a strip of grid points surrounding the mesh, the reduction factor being chosen to have the largest value on the grid boundary and taper gradually towards the centre of the grid. This gradual tapering is necessary to eliminate reflections.

Let $\Psi^{(m)}$ denote the wavefunction describing the system at the time step m. The absorbing effects are then described by the following scheme:

- solve the corresponding finite problem (calculation of $\Psi^{(m+1)}{}_{(0)}$ from $\Psi^{(m)}$)

- reduce the amplitude by the relation

$$\Psi^{(m+1)} = (1 - \gamma\tau)\Psi^{(m+1)}{}_{(0)} \tag{3}$$

where γ denotes the reduction function.

Kosloff & Kosloff [22] empirically found that for efficient absorption the derivative of γ should be kept as small as possible to avoid reflections, while on the other hand it should be large enough to eliminate transmission. Their choice for the spatial dependence for γ was chosen to be

$$\gamma = \frac{U_0}{cosh^2(\alpha k)} \tag{4}$$

where U_0 is a constant, α is the decay factor and k denotes the distance, in number of grid points, from the boundary.

7

Close examination of the above empirical absorbing scheme reveals that the function γ plays a similar role to a complex negative potential added to the Hamiltonian, as the amplitude reduction step can be derived from the equation

$$\frac{\partial \Psi}{\partial t} = -\gamma \Psi \tag{5}$$

with a first-order time propagation scheme. The one-dimensional NLS with the potential

$$\hat{V}(x) = \frac{U_0}{cosh^2(\alpha x)} \tag{6}$$

with U_0 real is a well-known model potential for which the transmission and reflection coefficients T and R have been worked out analytically [24]. The solutions can be modified in such a way as to obtain the values of the corresponding transmission and reflection coefficients, for the case of a complex potential as well [22].

The absorbing potential described above can be optimised by varying U_0 and α, to establish a balance between the number of grid points used for the absorbing region, and a sufficient reduction of the amplitude of the wave.

Ie. Present study

The present study follows the work of D. Griffiths, B. Herbst, A. Mitchell, J. Morris and Y. Tourigny [14] in solving the infinite NLS problem (similar studies concerning the numerical solution of the NLS can be found in [14, 15, 19, 20, 25, 30]). Given the appropriate initial conditions, soliton solutions are reconstructed, and the program's performance is tested for different values of the problem's free parameters. In particular, after examining the evolution of a single soliton form, collision between two solitons of different velocity have been considered, as well as the soliton formation from a non-soliton initial condition. The numerical method used is the well known *finite element* method, and the basis functions are the piecewise linear hat functions.

The absorption scheme (R. Kosloff and D. Kosloff [22]) is then applied to the right boundary, and the evolution of the single soliton form is again examined.

II. THE STUDY TOWARDS
THE NUMERICAL SOLUTION OF THE NLS

IIa. The finite element method

Consider the NLS equation together with the initial condition

$$u(x,0) = g(x) \qquad x_L \leq x \leq x_R$$

and the homogeneous Neumann (see [5]) boundary conditions

$$\left. \frac{\partial u}{\partial x} \right|_{x = x_L} = 0 \qquad ; \qquad \left. \frac{\partial u}{\partial x} \right|_{x = x_R} = 0 \qquad t > 0.$$

Setting

$$u(x,t) = v(x,t) + iw(x,t)$$

and

$$g(x) = g_R(x) + ig_I(x) \quad ,$$

the NLS leads to the system

$$\frac{\partial}{\partial t} \begin{pmatrix} v \\ w \end{pmatrix} + \begin{pmatrix} 0 & 1 \\ -1 & 0 \end{pmatrix} \frac{\partial^2}{\partial^2 x} \begin{pmatrix} v \\ w \end{pmatrix} + \lambda \begin{pmatrix} w(v^2 + w^2) \\ -v((v^2 + w^2) \end{pmatrix} = 0,$$

subject to the conditions

$$v(x,0) = g_R(x); \quad w(x,0) = g_I(x) \quad ,$$

and

$$\left. \frac{\partial v}{\partial x} = 0 \right|_{x = x_L, x_R} \qquad ; \qquad \left. \frac{\partial w}{\partial x} = 0 \right|_{x = x_L, x_R} \qquad .$$

It is convenient to denote

$$\vec{u} = (v,w)^T, \quad A = \begin{bmatrix} 0 & 1 \\ -1 & 0 \end{bmatrix}, \quad \vec{f}(\vec{u}) = (w(v^2 + w^2), -v(v^2 + w^2))^T$$

so that the equation takes the form

$$\frac{\partial \vec{u}}{\partial t} + A \frac{\partial^2 \vec{u}}{\partial x^2} + \lambda \vec{f}(\vec{u}) = \vec{0}.$$

Taking the L_2-inner product with elements of the space $H^1(x_L, x_R)$, integrating by parts, and using the boundary conditions,

$$\left(\frac{\partial \vec{u}}{\partial t}, \psi\right) - A\left(\frac{\partial \vec{u}}{\partial x}, \frac{\partial \psi}{\partial x}\right) + \lambda(\vec{f}, \psi) = \vec{0}, \qquad \forall \psi \in H^1(x_L, x_R).$$

The uniform mesh $x_L = x_1 < ... < x_N = x_R$ is then introduced, with

$$x_j - x_{j-1} = h, \qquad j = 2, 3, ..., N$$

and the piecewise linear 'hat' (or 'chapeau') functions are considered. These are denoted by ψ_j, $j = 1, \cdots, N$ and defined as follows:

$$\psi_j(x) = \begin{cases} (x - x_{j-1})/h, & x_{j-1} \leq x \leq x_j \\ (x_{j+1} - x)/h, & x_j \leq x \leq x_j + 1 \end{cases}, \qquad j = 2, 3, ..., N-1$$

$$\psi_1(x) = (x_2 - x)/h, \qquad x_1 \leq x \leq x_2$$

and

$$\psi_N(x) = (x - x_{N-1})/h, \qquad x_{N-1} \leq x \leq x_N \quad .$$

Suppose further that the approximation $\vec{U}(x, t)$ of the solution $\vec{u}(x, t)$, is given by the sum (see also R. Burden and D. Faires [5], I. Cristie [7])

$$\vec{U}(x, t) = \sum_{j=1}^{N} \vec{a}_j(t)\psi_j(x) \quad ,$$

where the time-dependent coefficients

$$\vec{a}_j(t) = (a_{j1}(t), a_{j2}(t))^T, \qquad j = 1, 2, ..., N$$

are to be determined. The discrete form of the NLS then given by the system

$$\sum_{j=1}^{N} \frac{d\vec{a}_j}{dt}(\psi_j, \psi_k) - A\sum_{j=1}^{N} \vec{a}_j(\frac{d\psi_j}{dx}, \frac{d\psi_k}{dx}) + \lambda(\vec{f}, \psi_k) = 0, \qquad k = 1, 2, ..., N.$$

The last term of the above equations is for the numerical calculations replaced by a product approximation, that is by a sum of the form:

$$(\vec{f}, \psi_k) \approx \sum_{j=1}^{N} \vec{f}(\vec{a}_j)(\psi_j, \psi_k).$$

Since $\psi_j(x)$ are the linear hat functions, direct calculation yields

$$(\psi_j, \psi_j) = \frac{2h}{3} \quad ; \quad (\psi_j, \psi_{j+1}) = (\psi_j, \psi_{j-1}) = \frac{h}{6}, \qquad j = 2, 3, ..., N-1$$

11

$$\left(\frac{\psi_j}{dx}, \frac{\psi_j}{dx}\right) = \frac{2}{h} \quad ; \quad \left(\frac{\psi_j}{dx}, \frac{\psi_{j+1}}{dx}\right) = \left(\frac{\psi_j}{dx}, \frac{\psi_{j-1}}{dx}\right) = \frac{-1}{h}, \quad j = 2, 3, ..., N-1$$

$$(\psi_1, \psi_1) = (\psi_N, \psi_N) = \frac{h}{3} \quad ,$$

and

$$\left(\frac{\psi_1}{dx}, \frac{\psi_1}{dx}\right) = \left(\frac{\psi_N}{dx}, \frac{\psi_N}{dx}\right) = \frac{1}{h}.$$

The final result is the following system of ordinary differential equations :

$$M\frac{d\vec{a}}{dt} + \frac{S}{h^2}\vec{a} + \lambda M\vec{F} = \vec{0} \quad , \tag{7}$$

where

$$M = \frac{1}{6}\begin{bmatrix} 2I & I & & 0 \\ I & 4I & I & \\ & & I & 4I & I \\ 0 & & & I & 2I \end{bmatrix}, \tag{8}$$

$$S = \begin{bmatrix} -A & A & & 0 \\ A & -2A & A & \\ & & A & -2A & A \\ 0 & & & A & -A \end{bmatrix}, \tag{9}$$

$$\vec{a} = (\vec{a}_1, \vec{a}_2, ..., \vec{a}_N)^T \tag{10}$$

and

$$\vec{F} = (\vec{F}_1, \vec{F}_2, ..., \vec{F}_N)^T \quad with \quad \vec{F}_j \equiv (\vec{a}_j^T \vec{a}_j) A\vec{a}_j. \tag{11}$$

The mass and stiffness matrices M and S are block tridiagonal symmetric matrices.

12

IIb. The numerical solution scheme

Infinite problem

In order to solve the system for $\vec{a}(t)$, the time interval is discretised by the grid points

$$t = m\tau, \qquad m = 0, 1, 2, \dots$$

where τ is the step size in time, and the scheme for the numerical solution is the following *predictor-corrector* pair :

$$M\vec{a}^* = (M - \frac{\tau}{h^2}S)\vec{a}^{(m)} - \tau\lambda M\vec{F}(\vec{a}^{(m)}) \tag{12}$$

$$(M + \frac{\tau}{2h^2}S)\vec{a}^{(m+1)} = M\vec{a}^{(m)} - \frac{\tau}{2h^2}S\vec{a}^{(m)} - \tau\lambda M\vec{F}\left(\frac{\vec{a}^* + \vec{a}^{(m)}}{2}\right) \tag{13}$$

The solution of the corrector formula for $\vec{a}^{(m+1)}$ is obtained by solving a system of linear equation of order $2N$, the coefficient matrix being the same at each time level. Consequently this matrix needs to be decomposed into its LU factors only once, and then for each new time level $m\tau$ ($m = 1, 2, \dots$) only a forward and backward substitution is required. This takes $12N$ operations (multiplications/additions) per time step, with an initial overhead of $18N$ operations for the LU decomposition. The procedure of solving for the $2N$ vector at each time step is therefore inexpensive.

Absorbing boundaries

For the implementation of the above predictor-corrector scheme in the case of absorbing boundaries, an extra step is required to include the absorbing effects, modifying the scheme as follows:

$$M\vec{a}^* = (M - \frac{\tau}{h^2}S)\vec{a}^{(m)} - \tau\lambda M\vec{F}(\vec{a}^{(m)}) \quad , \tag{14}$$

$$(M + \frac{\tau}{2h^2}S)\vec{a}^{(m+1)}_{(0)} = M\vec{a}^{(m)} - \frac{\tau}{2h^2}S\vec{a}^{(m)} - \tau\lambda M\vec{F}\left(\frac{\vec{a}^* + \vec{a}^{(m)}}{2}\right) \tag{15}$$

$$\vec{a}^{(m+1)} = (1 - \gamma\tau)\vec{a}^{(m+1)}_{(0)} \quad . \tag{16}$$

IIc. Solving linear systems in $\mathcal{R}^n$

The problem of solving a system of linear equations

$$A\vec{x} = \vec{b}, \quad A \in \mathcal{R}^{n \times n} \quad \vec{x}, \vec{b} \in \mathcal{R}^n$$

is central to the field of matrix computations. For the case where A is non-singular, the Gaussian method gives appropriate transformations $M_1, ..., M_{n-1} \in \mathcal{R}^{n \times n}$ such that

$$M_{n-1} \cdots M_2 M_1 A = U$$

where U is upper triangular, reducing the original $A\vec{x} = \vec{b}$ problem to the equivalent upper triangular system

$$U\vec{x} = (M_{n-1} \cdots M_2 M_1)\vec{b} \quad .$$

Suppose that for some $k < n$ Gauss transformations $M_1, ..., M_{k-1}$ have been determined such that

$$A^{(k-1)} \equiv M_{k-1} \cdots M_1 A = \begin{bmatrix} A_{11}^{(k-1)} & A_{12}^{(k-1)} \\ 0 & A_{22}^{(k-1)} \end{bmatrix} \begin{matrix} k-1 \\ n-k+1 \end{matrix}$$

$$\begin{matrix} k-1 & n-k+1 \end{matrix}$$

where $A_{11}^{(k-1)}$ is upper triangular. If

$$A_{22}^{(k-1)} \equiv \begin{bmatrix} a_{kk}^{(k-1)} & \cdots & a_{kn}^{(k-1)} \\ \vdots & & \vdots \\ a_{nk}^{(k-1)} & \cdots & a_{nn}^{(k-1)} \end{bmatrix}$$

and $a_{kk}^{(k-1)}$ is non-zero, then the multipliers

$$l_{ik} = \frac{a_{ik}^{(k-1)}}{a_{kk}^{(k-1)}} \qquad i = k+1, ..., n$$

are defined. It follows that if

$$M_k = I_k - \vec{l}^{(k)} e_k^T$$

where

$$\vec{l}^{(k)} \equiv (0, ..., 0, l_{k+1,k}, ..., l_{nk})^T \quad ,$$

then

$$A^{(k)} \equiv M_k A^{(k-1)} = \begin{bmatrix} A_{11}^{(k)} & A_{12}^{(k)} \\ 0 & A_{22}^{(k)} \end{bmatrix} \begin{matrix} k \\ n-k \end{matrix}$$
$$\begin{matrix} k & n-k \end{matrix}$$

with $A_{11}^{(k)}$ upper triangular and

$$(M_k \cdots M_1)^{-1} = M_1^{-1} \cdots M_k^{-1} = \prod_{i=1}^{k} (I_n + \vec{l}^{(i)} e_i^T) = I_n + \sum_{i=1}^{k} \vec{l}^{(i)} e_i^T \quad .$$

The theorem of *LU* decomposition states that given the non-singular matrix $A \in \mathcal{R}^{n \times n}$, there exists a unit lower triangular matrix $L \in \mathcal{R}^{n \times n}$ and an upper triangular matrix $U \in \mathcal{R}^{n \times n}$ such that $A = LU$. According to the calculations above $U = M_{n-1} \cdots M_2 M_1 A$ and also it is easy to prove that $L = M_1^{-1} \cdots M_{n-1}^{-1}$.

Once the *LU* decomposition of A has been computed there are two triangular systems remaining to be solved, namely the systems $L\vec{y} = \vec{b}$ and $U\vec{x} = \vec{y}$:

<u>Forward elimination</u> Given an $n \times n$ non-singular lower triangular matrix L, and the n-dimensional vector $\vec{b} \in \mathcal{R}^n$, find $\vec{y} \in \mathcal{R}^n$ such that $L\vec{y} = \vec{b}$:

For $i = 1, ..., n$
$\quad y_i \equiv b_i$
$\quad$ for $j = 1, ..., i-1$
$\quad\quad y_i \equiv y_i - l_{ij} y_j$
$\quad y_i \equiv y_i / l_{ii} \quad .$

<u>Back-substitution</u> Given an $n \times n$ non-singular upper triangular matrix U and the n-dimensional vector $\vec{y} \in \mathcal{R}^n$, find $\vec{x} \in \mathcal{R}^n$ such that $U\vec{x} = \vec{y}$:

For $i = 1, ..., n$
$\quad x_i \equiv y_i$
$\quad$ for $j = i+1, ..., n$
$\quad\quad x_i \equiv x_i - u_{ij} x_j$
$\quad x_i \equiv x_i / u_{ii} \quad .$

IId. *LU* decomposition in the NLS problem

Considering the matrices M and $(M + \tau/2h^2 S)$ of equations (12) and (13) it is convenient, for their factorisation, to take advantage of their tridiagonal structure. The systems to be solved can be written as

$$A \begin{bmatrix} \vec{a_1} \\ \vec{a_2} \\ \cdot \\ \cdot \\ \cdot \\ \vec{a_N} \end{bmatrix} = \begin{bmatrix} \vec{b_1} \\ \vec{b_2} \\ \cdot \\ \cdot \\ \cdot \\ \vec{b_N} \end{bmatrix}$$

where

$$A = \begin{cases} M \\ (M + \tau/2h^2 S) \end{cases},$$

and each of the $\vec{a_i}$'s and $\vec{b_i}$'s is a 2-dimensional vector. In either case matrix A can be written in the form

$$A \equiv \begin{bmatrix} D_1 & E & & 0 \\ E & D_2 & E & \\ & E & D_{N-1} & E \\ 0 & & E & D_N \end{bmatrix},$$

where each of the E's and D_i's is a 2×2 matrix. The system above has formally been solved [13] with the following results: If matrix A is denoted as a product of two triangular matrices, i.e. $A = LU$, then the lower-triangular matrix L will have the form

$$L = \begin{bmatrix} I & & 0 \\ L_2 & I & \cdot \\ 0 & L_N & I \end{bmatrix},$$

whereas the upper-triangular matrix U will have the form

$$U = \begin{bmatrix} U_1 & E & & 0 \\ & U_2 & E & \\ 0 & & & U_N \end{bmatrix},$$

where $L_i, U_i \in \mathcal{R}^{2 \times 2}$.

Solving for L_i and U_i the following algorithm is obtained,

$$U_1 = D_1$$
$$\text{for } i = 2, ..., N$$
$$\text{solve } L_i U_{i-1} = E \text{ for } L_i \quad,$$
$$U_i = D_i - L_i E \quad,$$

and having computed the components of the LU decomposition, the vector $\vec{a}$ is given via block forward elimination and back-substitution as follows :

$$\text{For } i = 1, ..., N$$
$$\vec{y}_i = \vec{b}_i - L_i \vec{y}_{i-1} \qquad (L_1 \vec{y}_0 \equiv 0) \quad,$$
$$\text{for } i = N, ..., 1$$
$$U_i \vec{a}_i = \vec{y}_i - E \vec{a}_{i+1} \qquad (E \vec{a}_{N+1} \equiv 0) \quad.$$

The triangular matrices L and U into which the matrix A is decomposed can always be obtained given the 2×2 diagonal matrices L_i, $i = 2, \cdots, N$ and U_i, $i = 1, \cdots, N$, calculated as above from the D_i's and E matrices.

For the decomposition of $A = (M + \tau/2h^2 S)$,

$$D_1 = D_N = \begin{bmatrix} 1/3 & -\tau/2h^2 \\ \tau/2h^2 & 1/3 \end{bmatrix} \quad,$$

$$D_i = \begin{bmatrix} 2/3 & -\tau/h^2 \\ \tau/h^2 & 2/3 \end{bmatrix}, \qquad for \quad i = 2, .., N-1$$

and

$$E = \begin{bmatrix} 1/6 & \tau/2h^2 \\ -\tau/2h^2 & 1/6 \end{bmatrix},$$

while in the case where $A = M$,

$$D_1 = D_N = \frac{1}{6} \begin{bmatrix} 2 & 0 \\ 0 & 2 \end{bmatrix} \quad,$$

$$D_i = \frac{1}{6} \begin{bmatrix} 4 & 0 \\ 0 & 4 \end{bmatrix}, \qquad for \quad i = 2, .., N-1$$

and

$$E = \frac{1}{6} \begin{bmatrix} 1 & 0 \\ 0 & 1 \end{bmatrix} \quad.$$

17

III. NUMERICAL EXPERIMENTATION

IIIa. Single Soliton

The algorithms described have been implemented into a computer program written in FORTRAN 77, and the numerical results were obtained in double-precision arithmetic.

A theoretical solution of the NLS with $\lambda = 1$ [32] is a complex valued function $u(x,t)$ representing a soliton travelling with velocity c in the positive direction of x. If its maximum modulus is taken to be $\sqrt{2a}$ the solution is given by the expression

$$u(x,t) = \sqrt{2a}\, exp\left[i\left(\frac{cx}{2} - \left(\frac{c^2}{4} - a\right)t\right)\right] sech\left[\sqrt{a}\,(x - ct)\right],$$

where a and c are positive constants. To test a numerical solution, the NLS is subjected to the initial condition

$$u(x,0) = \sqrt{2a}\, exp\left(\frac{icx}{2}\right)\; sech\left(\sqrt{a}x\right),$$

with natural boundary conditions at $x = x_L$ and $x = x_R$, for all $t > 0$. In the numerical calculations $[x_L, x_R] = [-30, 70]$.

The program is tested successfully for different values of the velocity c and for an amplitude $a = 0.5$. The space and time intervals are chosen to be $[h = 0.5, \tau = 0.15]$. Best results were obtained for $0.2 < c < 2.2$.

The initial form of the soliton is shown in figure Ia, while figures Ib up to Id, show the position of the soliton after $t = 20$, $t = 40$ and $t = 60$ iteration steps respectively, and for a soliton velocity $c = 1.0$.

Figures Ie and If have been made to test the program's performance for different soliton velocities as well, namely for $c = 0.5$ and $c = 1.5$. Here a 'snapshot' of the soliton form is taken at the time step of 40 iterations.
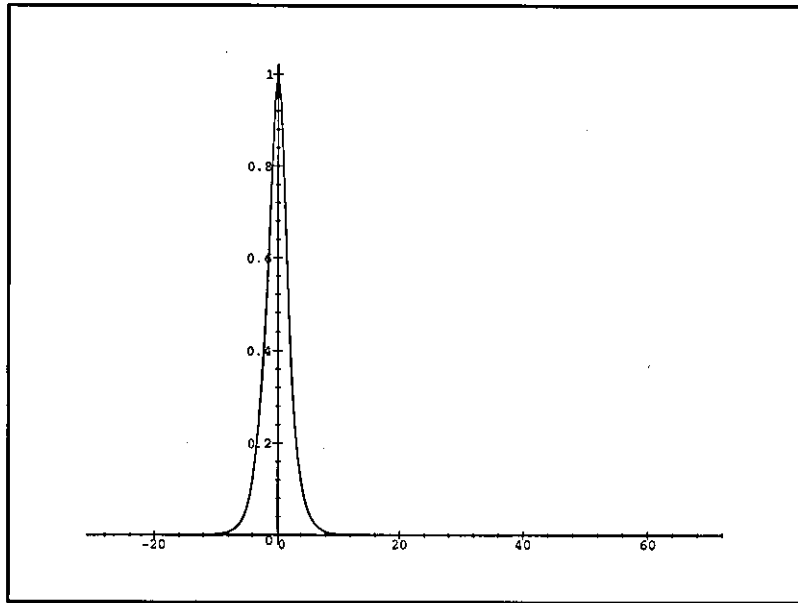
Figure Ia.
Soliton's initial position ($t = 0$).

Figure Ib.
Soliton's position for time $t = 20$ - Soliton's velocity $c = 1.0$.

19

Figure Ic.
Soliton's position for time $t = 40$ - Soliton's velocity $c = 1.0$.

Figure Id.
Soliton's position for time $t = 60$ - Soliton's velocity $c = 1.0$.
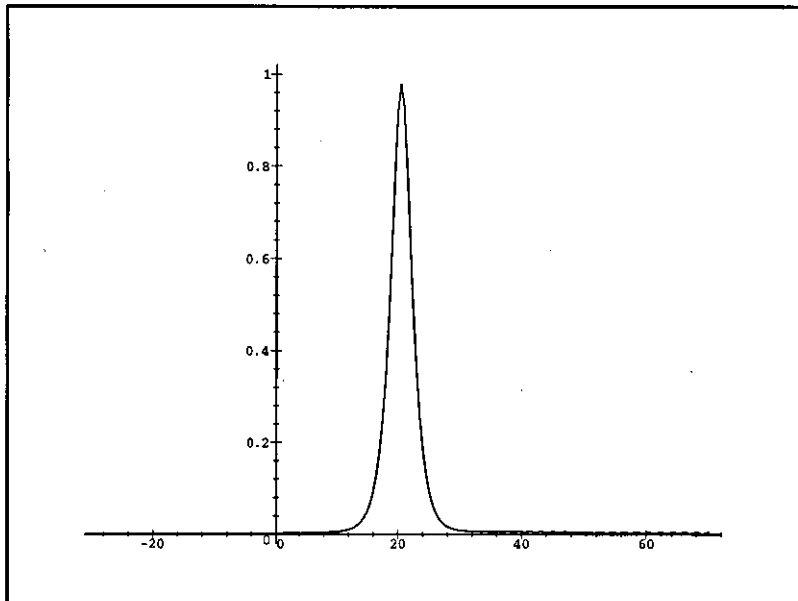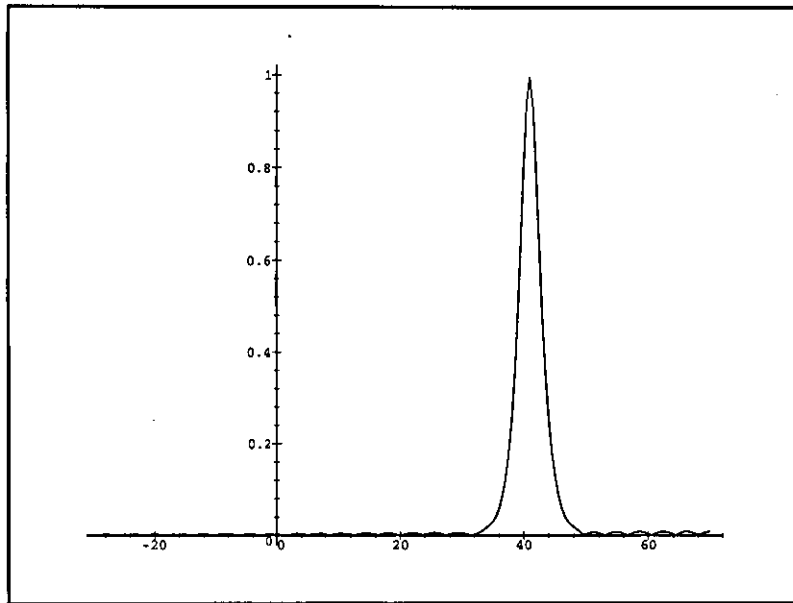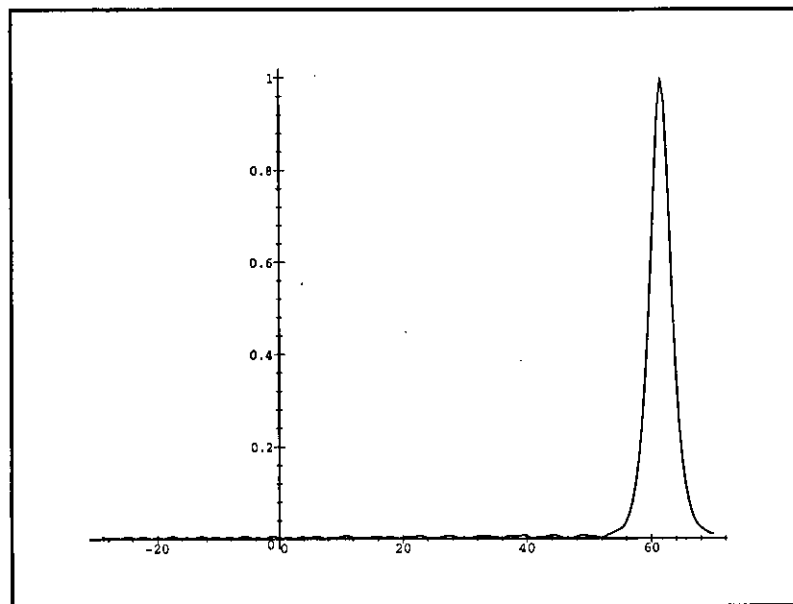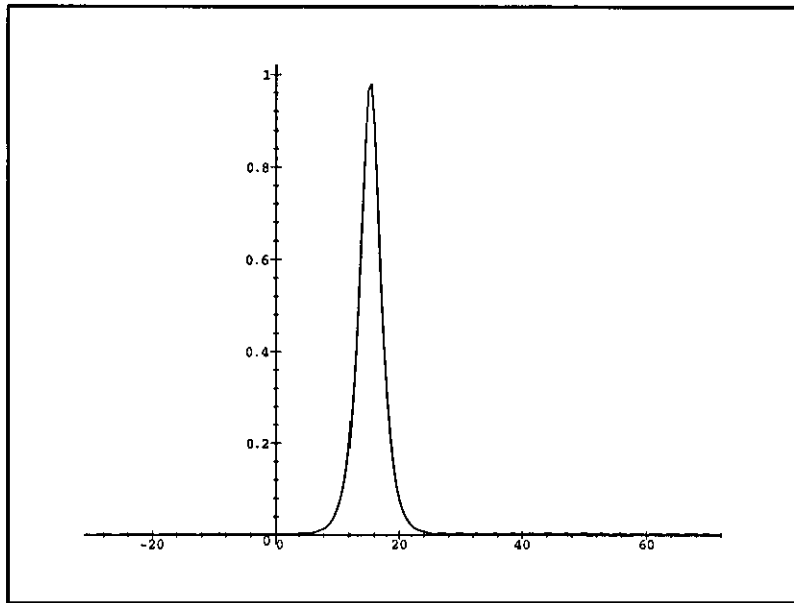
20

Figure Ie.
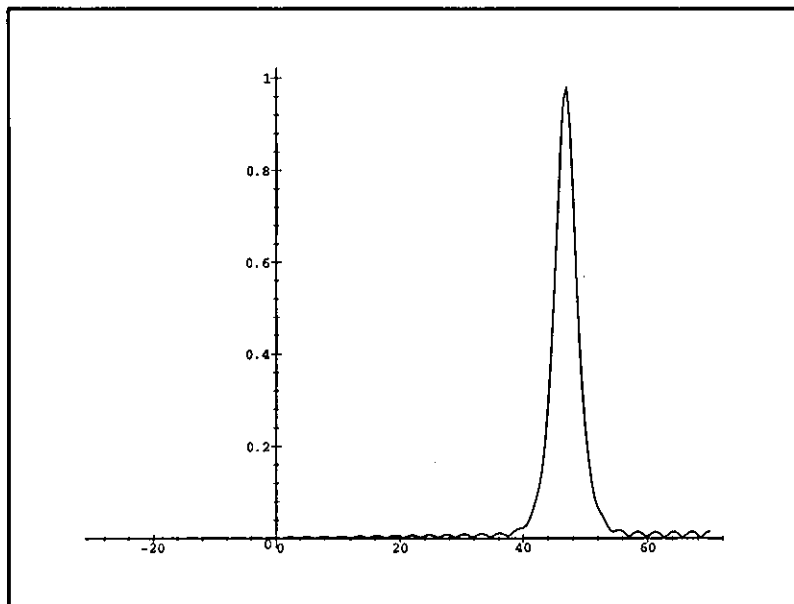Soliton's position for time $t = 40$ - Soliton's velocity $c = 0.5$.

Figure If.
Soliton's position for time $t = 40$ - Soliton's velocity $c = 1.5$.

21

IIIb. Collision of Two Solitons

Now the NLS is given the initial condition

$$u(x,0) = \sqrt{2a}\left[exp\left(\frac{ic_1x_1}{2}\right)sech\left(\sqrt{a}x_1\right) + exp\left(\frac{ic_2x_2}{2}\right)sech\left(\sqrt{a}x_2\right)\right],$$

where $c_1 > c_2$, $x_1 \equiv x$ and $x_2 \equiv x - 25$, representing in fact two soliton forms separated by a distance equal to 25 units. The faster wave (velocity c_1) is situated initially at $x = 0$, while the slower wave (velocity c_2) is situated at $x = 25$. As time progresses the faster wave ultimately catches the slower one, and theoretically passes through it with only a phase shift as a result. The boundary conditions imposed here are again natural and $[x_L, x_R] = [-20, 80]$.

In order for a reasonable interaction to occur, the velocities are chosen to be $c_1 = 1.0$ and $c_2 = 0.1$. The resulting profiles have been computed up to $t_{max} = 50$, time which allows the fast moving soliton to overtake and interact with the slow moving one. There is also enough time for the subsequent solitons to move apart after the interaction. The parameter set is again chosen to be $[h = 0.5, \tau = 0.15]$.

Figure IIa shows the initial position of the two waves, while figures IIb to IIf show the evolution of the two soliton forms in time. 'Snapshots' are taken for $t = 10$, $t = 20$, $t = 30$, $t = 40$ and $t = 50$ iterations. The solitons can be observed to travel towards each other, interact and move apart, finally regaining their initial form. Figures IIg to IIj show the sensitivity of the program on the choice of the parameters τ and h. The five different combinations of these parameters (which are the same as the ones used in the tests of [14]) are given in the following table.

Figure	τ	h
IIg	0.06125	0.25
IIh	0.04167	0.3333
IIi	0.125	0.5
IIj	0.125	0.25

As can be observed, the combinations which give best results after the time of 50 iterations are those used in figures IIg and IIj, for the smallest choice of the space interval h ($h = 0.25$).
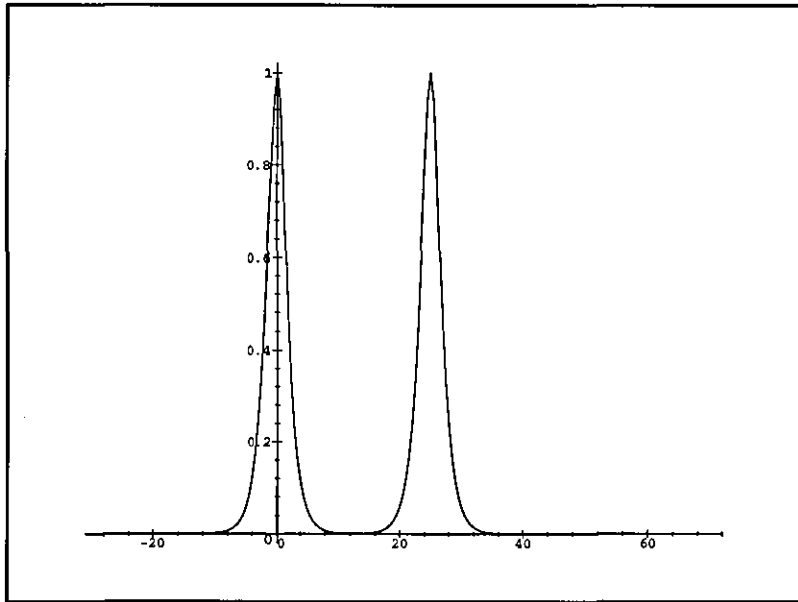
Figure IIa.
Initial position of the two solitons $(t = 0)$.
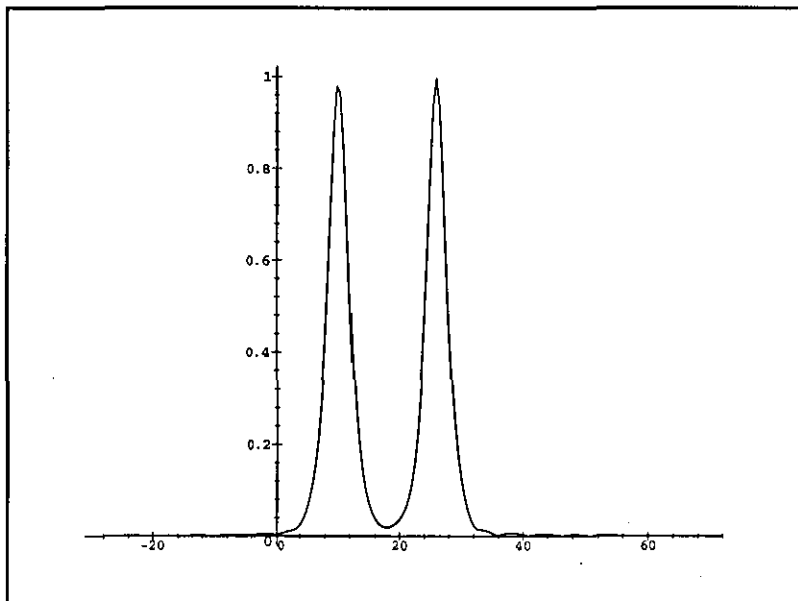
Figure IIb.
Evolution of the two soliton forms, $t = 10$.

23

Figure IIc.
Evolution of the two soliton forms, $t = 20$.

Figure IId.
Evolution of the two soliton forms, $t = 30$.

24

Figure IIe.
Evolution of the two soliton forms, $t = 40$.

Figure IIf.
Evolution of the two soliton forms, $t = 50$.

Figure IIg.
Evolution of the two soliton forms, $t = 50$, $\tau = 0.06125$, $h = 0.25$.

Figure IIh.
Evolution of the two soliton forms, $t = 50$, $\tau = 0.04167$, $h = 0.3333$.

Figure IIi.
Evolution of the two soliton forms, $t = 50$, $\tau = 0.125$, $h = 0.5$.

Figure IIj.
Evolution of the two soliton forms, $t = 50$, $\tau = 0.125$, $h = 0.25$.

IIIc. Non-soliton initial data

From the theoretical investigations of the NLS equation (2), the case of $\lambda = 1$, which is the case under study in the present report, is known as the *focusing case* [11], as it allows soliton formation as time evolves. In the *de-focusing case* $\lambda = -1$, no soliton solutions can be said to be formed.

The aim of the present section is to investigate the effect of non-soliton initial data with $\lambda = 1$. Given non-soliton initial conditions, the solution of the NLS is expected to include soliton formations which evolve with time. It is worth noticing here that the exact number, or shape, of the solitons in the solution when $t \to \infty$, can not be predicted.

The NLS given the non-soliton initial condition

$$v(x,0) = exp\left(-0.1x^2\right)$$

$$w(x,0) = -x\,exp\left(-0.1x^2\right)$$

and natural boundary conditions at $[x_L, x_R] = [-80, 20]$, the following numerical results were obtained:

The initial form of the wave is given in figure IIIa. Figures IIIb to IIId show the evolution of the waveform for the successive times of 20, 30 and 40 iterations and for the choice of parameters $[\tau = 0.015625, h = 0.125]$. As can be observed from the figures, there are two main solitary waves being formed together with several waves of smaller amplitude, evolving to the left as time increases.

Two more combinations of τ and h have been tested and the results at the time of 40 iterations are presented in figures IIIe and IIIf, according to the following table:

Figure	τ	h
IIIe	0.03125	0.25
IIIf	0.015625	0.25

It is worth noticing that the formation of the several solitons can be said to be more clearly shown when the smaller space interval ($h = 0.125$) is used ((figures IIIb-IIId) and also when the time-interval has its smaller value ($\tau = 0.015625$, Figure IIIf).

28
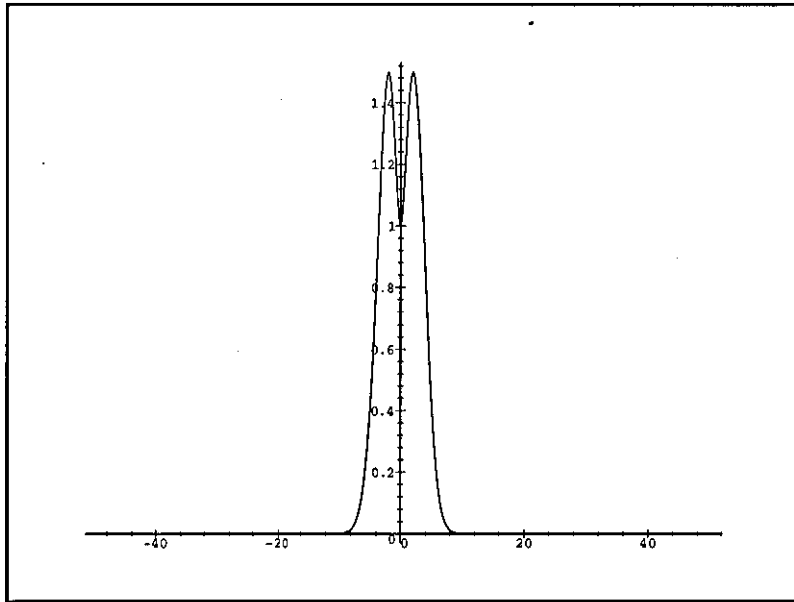
Figure IIIa.
Initial position of the non-soliton form ($t = 0$).
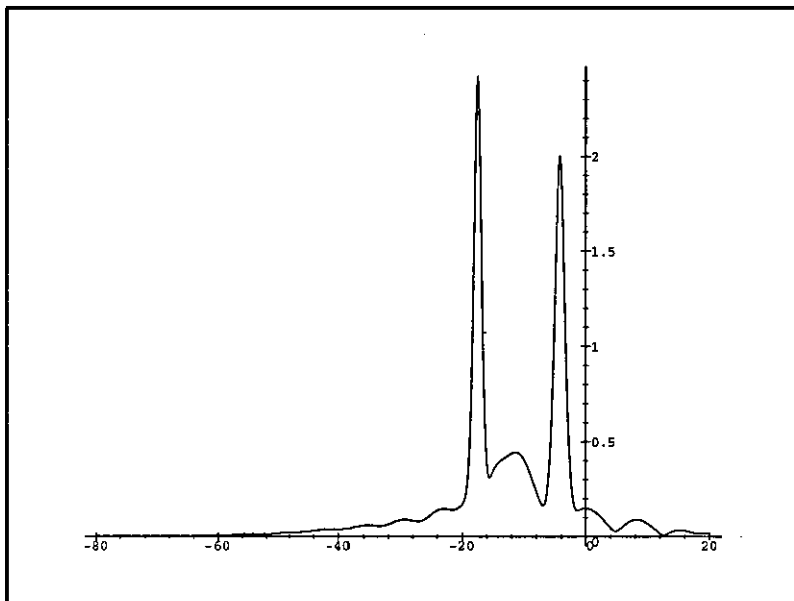
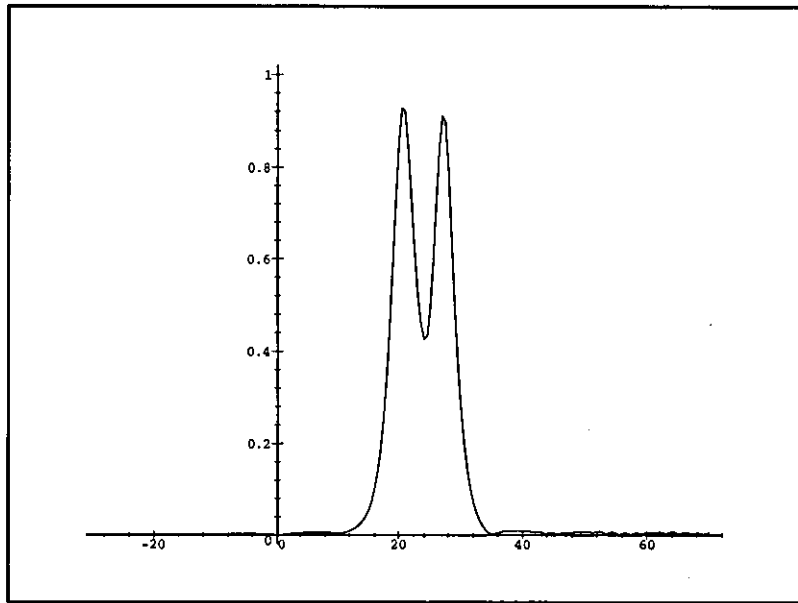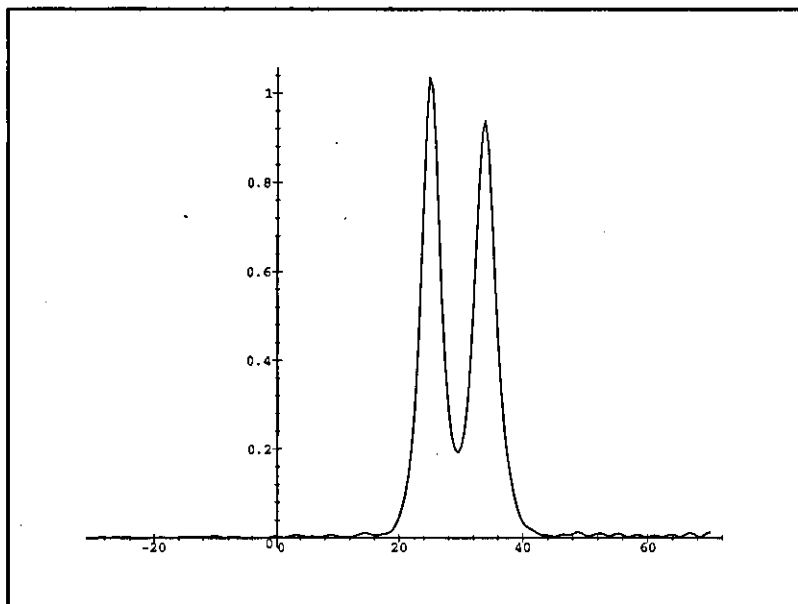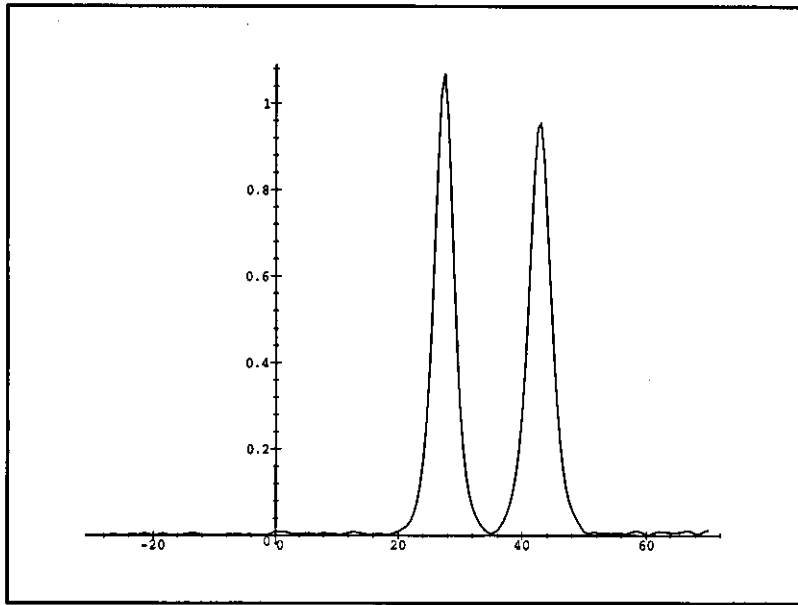Figure IIIb.
Evolution of the non-soliton form, $t = 20$.

29
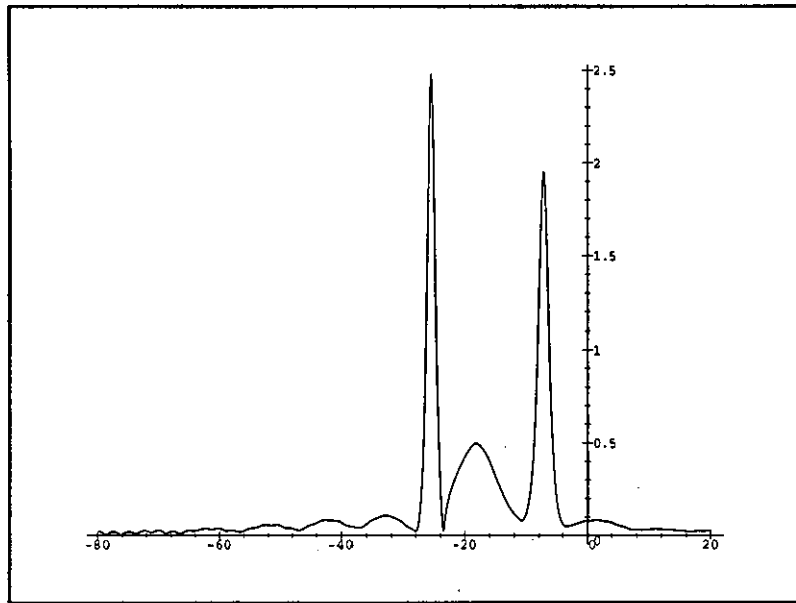
Figure IIIc.
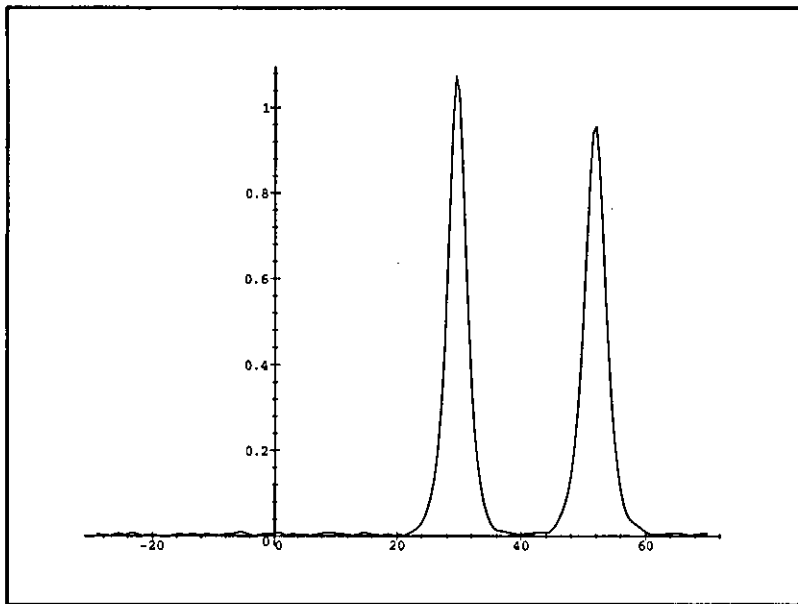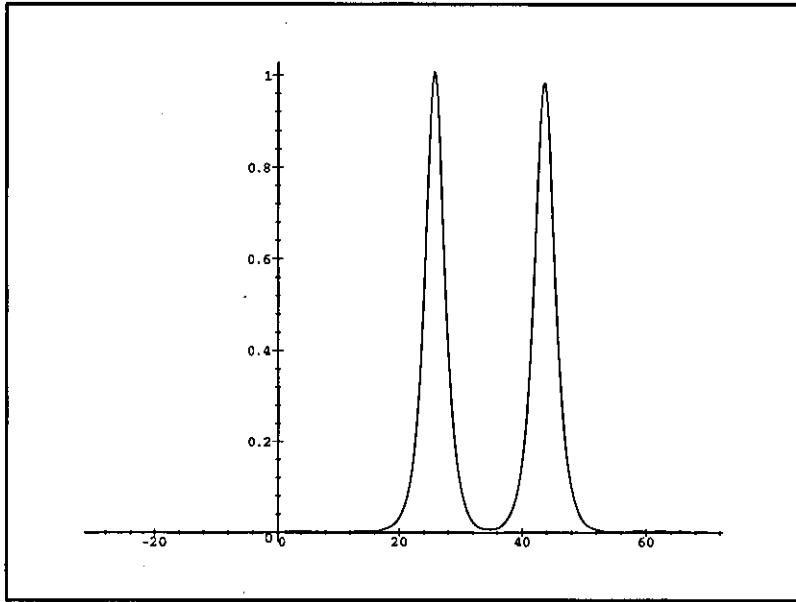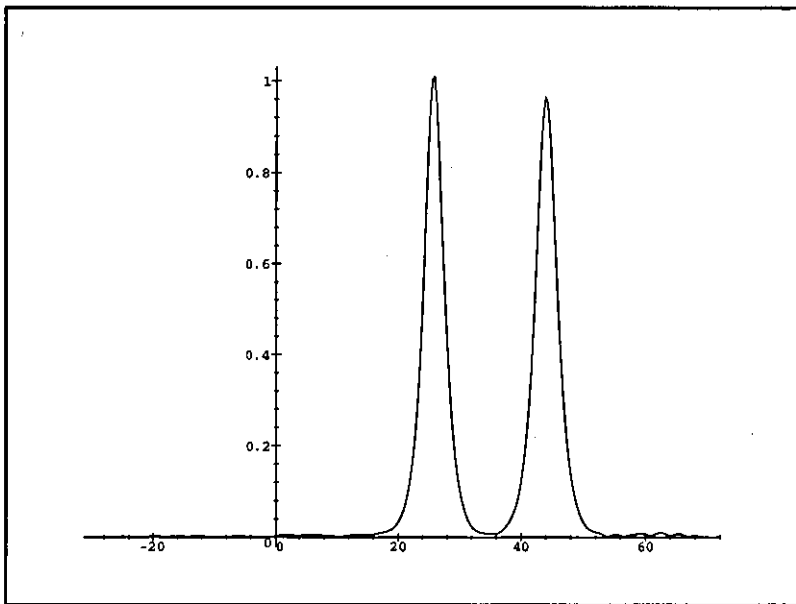Evolution of the non-soliton form, $t = 30$.
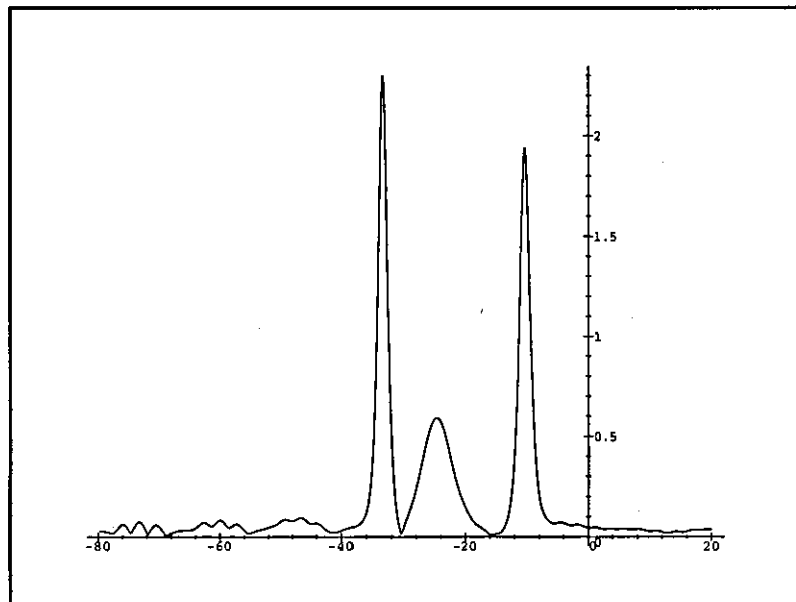
Figure IIId.
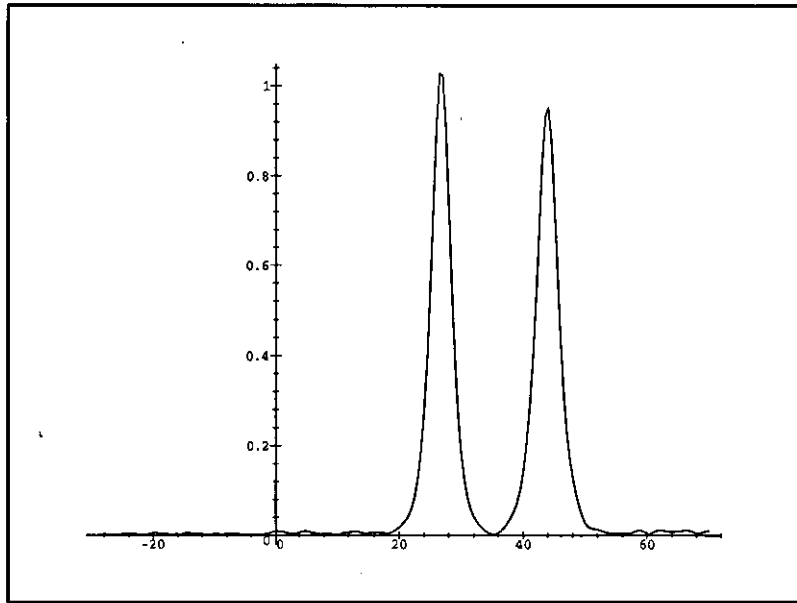Evolution of the non-soliton form, $t = 40$.
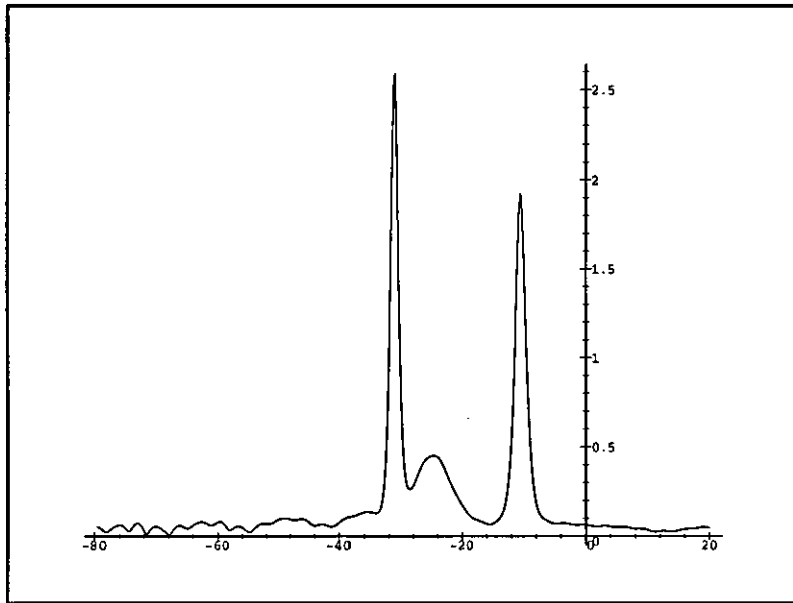
Figure IIIe.
Evolution of the non-soliton form, $t = 40$, $\tau = 0.03125$, $h = 0.25$.
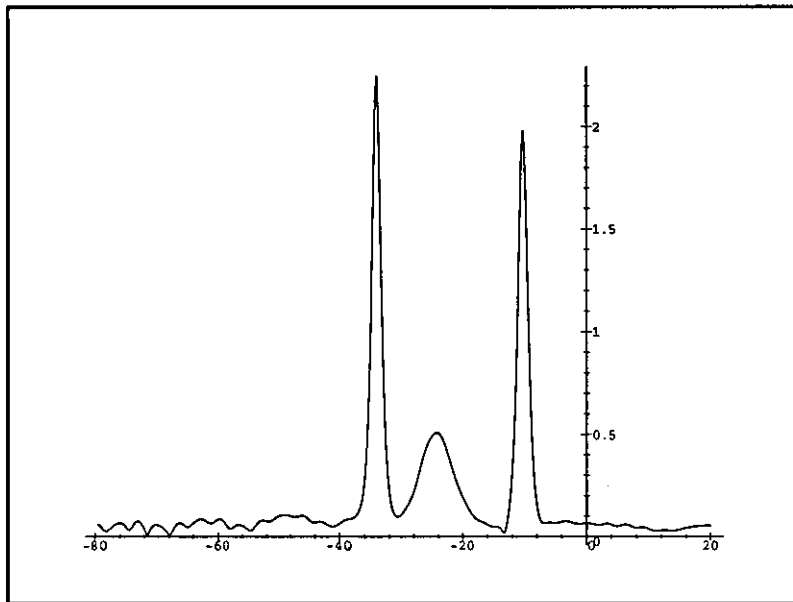
Figure IIIf.
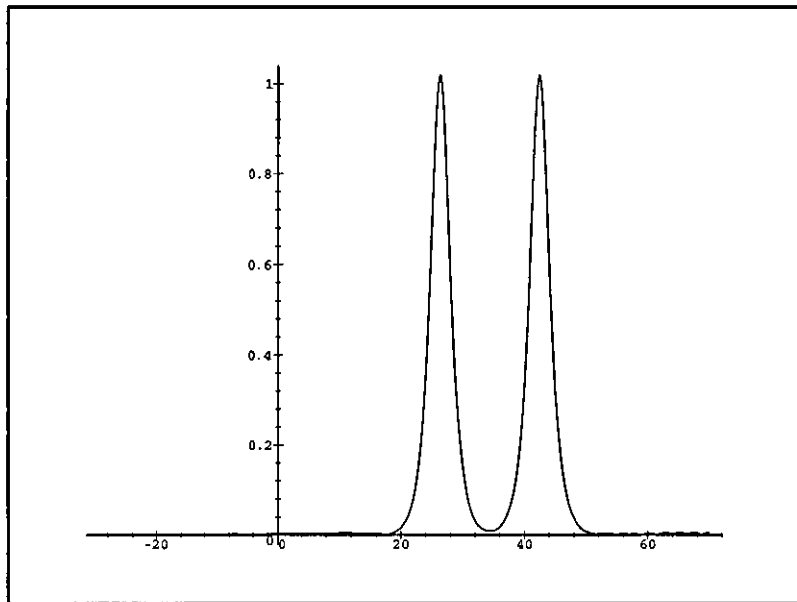Evolution of the non-soliton form, $t = 40$, $\tau = 0.015625$, $h = 0.25$.

31

IIId. Implementation of the absorbing boundaries

In these tests the initial condition is the one-soliton form of section IIIa, traveling with a velocity of $c = 1.0$. The important effects of the implementation of the absorbing boundaries are clear in figures IVa up to IVd, where the soliton can be seen to travel very close to the right boundary x_R. Snapshots of the waveform are taken at the successive times of 60, 65, 70 and 80 iterations. It is easy to observe that when the waveform reaches the boundary region it is eliminated without noticeable reflection from it.

Following a trial and error procedure, and after a number of tests using different combinations for the two parameters, best absorbing results were obtained for the parameter choice $U_0 = 0.4$ and $\alpha = 0.18$.
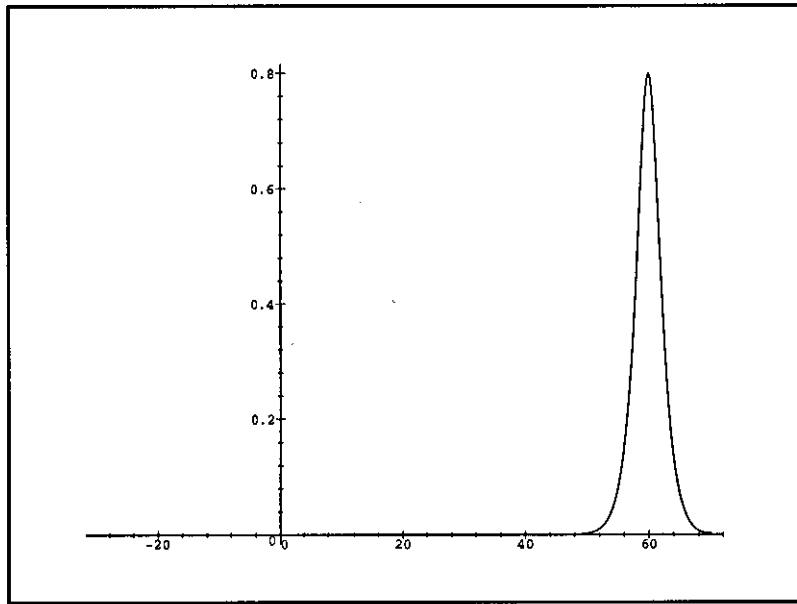
Figure IVa.
Absorbing boundaries - Soliton's position for $t = 60$.
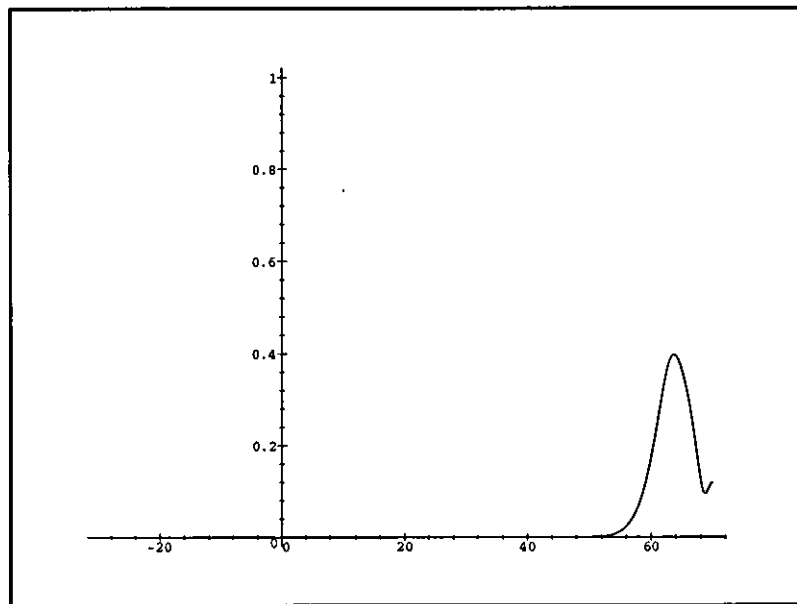
Figure IVb.
Absorbing boundaries - Soliton's position for $t = 65$.
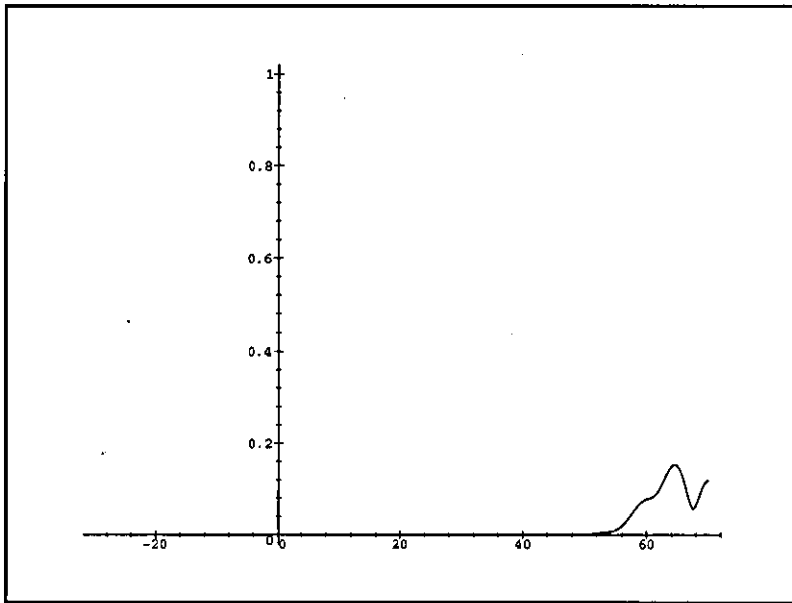
Figure IVc.
Absorbing boundaries - Soliton's position for $t = 70$.
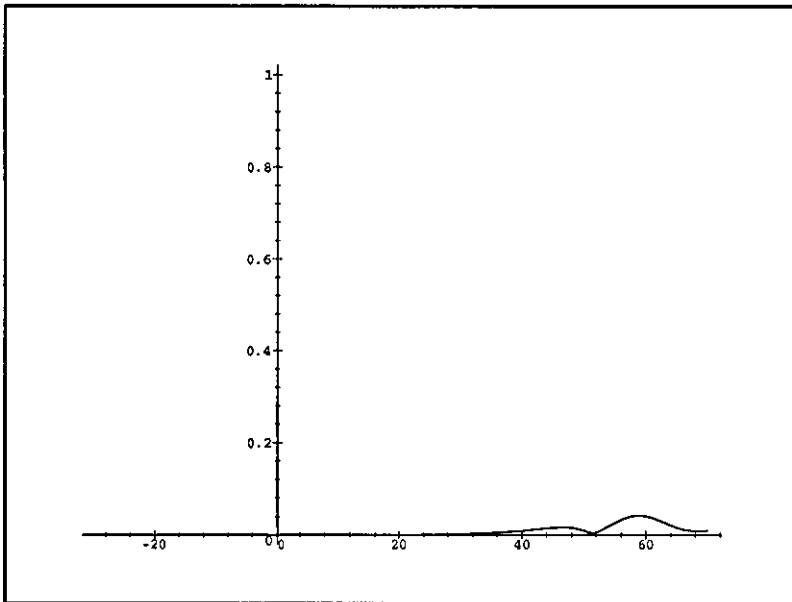
Figure IVd.
Absorbing boundaries - Soliton's position for $t = 80$.

IV. CONCLUSION

The solution of the NLS equation (2) for $-\infty < x < \infty$ and for $t > 0$ is approximated by a sum of the linear "hat" functions $\psi_j(x)$, defined on the interval $[x_L, x_R]$. Denoting $\vec{U}(x,t) = \sum_{j=1}^{N} \vec{a}_j(t)\psi_j(x)$ the numerical approximation of the solution, the (2×1) coefficients $\vec{a}_j(t)$ are time-dependent and are elements of the $(2N \times 1)$ vector $\vec{a}$, which is the solution of the predictor-corrector scheme of equations (12) and (13).

Given the initial conditions, the numerical approximation $\vec{U}(x,t)$ of the solution inside the numerical grid $[x_L, x_R]$ is considered to be satisfactory, provided that $[x_L, x_R]$ is sufficiently large and that the final time t_f for the calculation of $\vec{U}(x, t_f)$ is small enough to avoid reflections from the boundaries of the grid.

Given the appropriate initial conditions, the chosen numerical method efficiently simulates the evolution of one soliton form travelling with different velocities (figures Ia - If), the collision of two solitons (figures IIa - IIj), and also clearly shows the soliton formation for non-soliton initial data (figures IIIa - IIIf). As expected, best results were obtained for the smallest choice of the space and time parameters h and τ. It is worth noticing though that, according to the initial condition, an optimum combination $[h_o, \tau_o]$ of these parameters can be found, so that $\forall (h < h_o, \tau < \tau_o)$ the calculated approximation of the solution is not essentially improved.

The absorption scheme described in section Id is found, in its implementation, to successfully eliminate the effects from the boundaries of the numerical grid (figures IVa - IVd). Provided that the choice of the absorption parameters $[U_0, \alpha]$ given in section IIId is optimal (the proposed parameter set was found after a trial and error procedure), the problem of the NLS (2) can also be solved numerically for sufficiently large times. This makes the numerical solution scheme more flexible, as far as the choice of the space interval $[x_L, x_R]$ and the final time t_f is concerned. In addition, the modified predictor-corrector equations (14) - (16) can be said to be satisfactory for the study of the infinite problem, regardless of the given initial condition.

PART TWO

Dynamical Systems

And

Bifurcations Of Vector Fields

I. INTRODUCTION

Ia. Bifurcation theory - A review

The word *bifurcation* includes the idea of division into two parts. In mathematics it is used in a wide sense to indicate every qualitative topological metamorphosis occurring under the variation of parameters on which a dynamical system depends. The objects under study can be real or complex curves or surfaces, functions or mappings, manifolds, vector fields or equations.

The tremendous development bifurcation theory has recently undergone, has to deal with an infusion of new ideas and methods, ranging from dynamical systems theory, group theory, and computer-assisted studies of dynamics. Arnold ([2]) with the following characterisation, reflects the broadness of the subject: "The word bifurcation, meaning some sort of branching process, is widely used to describe any situation in which the qualitative, topological picture of the object we are studying, alters with a change of the parameter on which the object depends. The objects in question can be extremely diverse: for example, real or computer curves or surfaces, functions or maps, manifolds or fibrations, vector fields, differential or integral equations".

The aim of bifurcation theory is the study of the qualitative changes in the phase portrait, these being either appearances or disappearances of equilibria, periodic orbits, or even more complicated features such as strange attractors. As a general theory, bifurcation is able to give results proven to be fundamental to the understanding of non-linear dynamical systems, but also successfully applicable to any area of non-linear physics.

The present study deals with dynamical systems in the form of differential equations, often arising in the modelling of physical systems and in particular when trying to formulate the equations describing the system. A point $\vec{x}$ in the phase space of the system corresponds to a system's possible state, and the given initial condition of the system's characteristic differential equation defines a curve in phase space passing through $\vec{x}$. The collective representation of these curves for all points in phase space is the so-called *phase portrait*, which in fact provides a global qualitative picture of the system's dynamics and depends on any parameters that appear in the equations of motion. When these parameters vary,

the phase portrait may deform slightly without its qualitative features being altered. However, there is the possibility of a qualitative change, whenever there is a significant modification in the system's dynamics.

In the sections that follow, elementary aspects of bifurcation theory are presented, including fundamentals and general assumptions, as well as brief descriptions of the different possible bifurcations. The study closely follows the work of J. Crawford [6], though V. Arnold's work on geometrical methods in the theory of ordinary differential equations [3], as well as J. Guckenheimer's study of dynamical systems [17] also provided considerable help towards the understanding of the finer points of the study.

Ib. The theory's basic features

Consider dynamical processes defined by autonomous, first order systems of the form

$$\dot{\vec{x}} = \vec{V}(\mu, \vec{x}) \quad , \qquad \vec{x} \in \mathcal{R}^n, \qquad \mu \in \mathcal{R}, \qquad (17)$$

which depend on the parameter μ and describe the motion in an n-dimensional phase space $\mathcal{R}^n$. Formulated this way a differential equation is identified with the vector field $\vec{V}(\mu, \vec{x})$ on $\mathcal{R}^n$, while in the same way, given the vector field one can always define the associated differential equation.

In a dynamics that represents the evolution of a system at discrete time intervals, the motion is described by a *map* [6], that is by a relation of the form

$$\vec{x}_{j+1} = \vec{f}(\mu, \vec{x}_j) \quad , \qquad for \qquad j = 0, 1, 2, \cdots, \quad \vec{x} \in \mathcal{R}^n, \quad \mu \in \mathcal{R}, \quad (18)$$

where the index j labels successive points in the trajectory.

The dynamical systems defined by maps and those defined by vector fields are very closely connected. The solutions of equation (17) may also be given as trajectories: an initial condition $\vec{x}(0)$ determines uniquely a solution $\vec{x}(t)$ and the corresponding curve in $\mathcal{R}^n$, parametrised by t, is the trajectory of $\vec{x}(0)$.

From a more abstract point of view, this association $\vec{x}(0) \longrightarrow \vec{x}(t)$ defines the mapping

$$\phi_t : \mathcal{R}^n \to \mathcal{R}^n$$

where $\phi_t(\vec{x}(0)) \equiv \vec{x}(t)$. This mapping is called the *flow* [6] determined by equation (17).

Ic. Present study

Whether one is dealing with flows or maps, it is characteristic that the dynamics, in either case be allowed to depend on an adjustable parameter μ. The origin $(\mu, \vec{x}) = (0, 0)$ is assumed to be the equilibrium point for the motion, as

$$\vec{V}(0, 0) = 0,$$

or equivalently

$$\vec{f}(0, 0) = 0,$$

noticing that, given an equilibrium solution at (μ_0, x_0), it can always be moved to the origin by an appropriate change of coordinates (see also [3, 6, 17]).

Bifurcation theory investigates what happens in the phase space near $\vec{x} = 0$, in case where there are variations about $\mu = 0$. The key observation by which one can proceed to the study of the non-linear case is that the problem can be reduced to a system of linear equations to be solved, namely a Taylor series for the vector field, containing only the essential terms. For bifurcation theory one is specifically interested in equilibria at which there are eigenvalues with zero real parts for the matrix corresponding to the linearised system. At such equilibria the linearisation problem cannot be solved, and there are terms in the linear matrix which cannot be removed by coordinate changes. This can result in the stability of equilibria near $\mu = 0$ leading to different forms of bifurcation, or different types of changes in the number of solutions for the given differential equation.

The present study, after overviewing the theory's basic features for the linear and the non-linear dynamics, deals with the simplest bifurcations of equilibria for either the case of flows or maps.

II. THE THEORY'S BASIC FEATURES

IIa. Linearisation in flows

The present section closelly follows the work of J. Crawford in [6], as well as the work of J. Guckenheimer in [17]. Considering $\vec{x} = 0$, and taking the Taylor expansion of equation (17),

$$\dot{\vec{x}} = \vec{V}(\mu, 0) + D\vec{V}(\mu, 0)\,\vec{x} + \mathcal{O}(|\,\vec{x}\,|^2)\quad,$$

where $D\vec{V}(\mu, 0)$ represents the square matrix with elements

$$\left(D\vec{V}(\mu, 0)\right)_{ij} \equiv \frac{\partial V_i}{\partial x_j}(\mu, 0)\quad,$$

and the term $\mathcal{O}(|\,\vec{x}|^2)$ includes the higher order terms, that are at least quadratic in the components of $\vec{x}$.

At $\mu = 0$ the constant term of the Taylor expansion vanishes and, ignoring the non-linear term we get the following linearised system:

$$\dot{\vec{x}} = D\vec{V}(0, 0)\,\vec{x}\quad. \tag{19}$$

Considering a typical situation, the eigenvalues of $D\vec{V}(0, 0)$ are non-degenerate and the matrix above can be diagonalised by a linear change of coordinates $\vec{x} \to \tilde{\vec{x}}$, allowing equation (19) to be re-expressed in the form

$$\frac{d}{dt}\begin{bmatrix} \tilde{x}_1 \\ \tilde{x}_2 \\ \cdot \\ \cdot \\ \cdot \\ \tilde{x}_n \end{bmatrix} = \begin{bmatrix} \lambda_1 & 0 & \cdots & 0 \\ 0 & \lambda_2 & & \cdot \\ \cdot & & & \cdot \\ \cdot & & & 0 \\ 0 & \cdots & 0 & \lambda_n \end{bmatrix} \begin{bmatrix} \tilde{x}_1 \\ \tilde{x}_2 \\ \cdot \\ \cdot \\ \cdot \\ \tilde{x}_n \end{bmatrix} \quad,$$

with a general solution

$$\tilde{\vec{x}}(t) = \begin{bmatrix} \tilde{x}_1(0)e^{\lambda_1 t} \\ \tilde{x}_2(0)e^{\lambda_2 t} \\ \cdot \\ \cdot \\ \cdot \\ \tilde{x}_n(0)e^{\lambda_n t} \end{bmatrix} \quad.$$

41

Notice that if $\mathcal{R}e(\lambda_i) < 0$, then as $t \to \infty$ the $\tilde{x}_i$ component decays to zero. Conversely the case $\mathcal{R}e(\lambda_i) > 0$ implies exponentially rapid growth of $\tilde{x}_i$.

For each eigenvalue λ of $D\vec{V}(0,0)$ there is an associated linear subspace of $\mathcal{R}^n$, the so-called *eigenspace* E_λ. Assuming that $D\vec{V}(0,0)$ is diagonalisable in respect to λ, the definition of E_λ depends only on whether λ is complex or real in the following way :

If λ is real, E_λ is simply the subspace spanned by the eigenvectors

$$E_\lambda \equiv \{\vec{v} \in \mathcal{R}^n | \ (D\vec{V}(0,0) - \lambda I)\, \vec{v} = 0\}, \quad \lambda \in \mathcal{R} \quad ,$$

and if λ is non-degenerate *dim* $E_\lambda = 1$.

If λ is complex the eigenvectors are also complex and their real and imaginary parts span the eigenspace E_λ. If $\vec{v}_1 + i\vec{v}_2$ is such an eigenvector for λ then the complex conjugated vector $\vec{v}_1 - i\vec{v}_2$ is an eigenvector for $\bar{\lambda}$, and the above definition of the eigenspace can be replaced by the relation

$$E_\lambda \equiv \{\vec{v} \in \mathcal{R}^n | \ (D\vec{V}(0,0) - \lambda I)(D\vec{V}(0,0) - \bar{\lambda} I)\, \vec{v} = 0\}, \quad \lambda \in \mathcal{C}^n \quad .$$

Now *dim* $E_\lambda = 2$, if λ is non-degenerate.

When $D\vec{V}(0,0)$ has eigenvalues that are degenerate, the above construction for E_λ remains satisfactory, provided $D\vec{V}(0,0)$ is diagonalisable. In case this doesn't happen, the eigenspace definitions must be extended to include generalised eigenvectors as well.

An eigenvalue λ corresponds to a *mode* of the system that is stable, unstable, or neutral, depending on whether $\mathcal{R}e(\lambda) < 0$, $\mathcal{R}e(\lambda) > 0$, or $\mathcal{R}e(\lambda) = 0$ respectively. Thus the eigenvectors of $D\vec{V}(0,0)$ are divided into three sets, according to these three possibilities, leading to the formation of
the *stable subspace* E^s,

$$E^s \equiv span\{\vec{v}| \ \vec{v} \in E_\lambda \quad and \quad \mathcal{R}e(\lambda) < 0\} \quad ,$$

the *unstable subspace* E^u,

$$E^u \equiv span\{\vec{v}| \ \vec{v} \in E_\lambda \quad and \quad \mathcal{R}e(\lambda) > 0\} \quad ,$$

and the *centre subspace* E^c,

$$E^c \equiv span\{\vec{v}| \ \vec{v} \in E_\lambda \quad and \quad \mathcal{R}e(\lambda) = 0\} \quad .$$
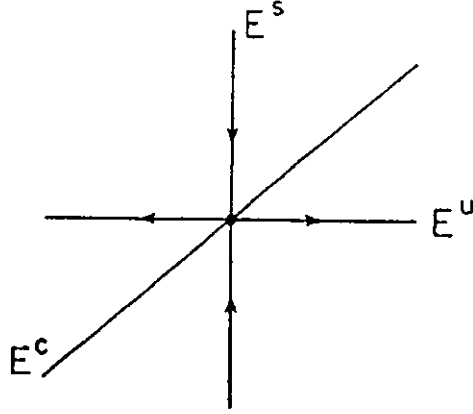
Figure Va. Invariant linear subspaces E^s, E^u, E^c.

The subspaces above span the phase space $\mathcal{R}^n = E^s \oplus E^c \oplus E^u$ and they are invariant under (19) as, if $\vec{x}(0) \in E^\alpha$, the trajectory $\vec{x}(t) \in E^\alpha$ (where $\alpha = s, c, u$). The asymptotic dynamics of E^s and E^u are simple: If $\vec{x}(t) \in E^s$ then as $t \to \infty$, the trajectory converges to the equilibrium, while if $\vec{x}(t) \in E^u$ the trajectory converges to the equilibrium as $t \to -\infty$. Figure Va illustrates the above features. The same figure can be found in [6], as well as figures Vb-Vj of the present work.

Definition

An equilibrium at $\vec{x} = 0$ is asymptotically stable, if there exists a neighbourhood of initial conditions $0 < |\vec{x}(0)| < \varepsilon$ such that, for all $\vec{x}(0)$ in this neighbourhood the trajectory $\vec{x}(t)$ satisfies $|\vec{x}(t)| < \varepsilon$, for $t > 0$, and $|\vec{x}(t)| \to 0$ as $t \to \infty$.

For the linear system of equation (19) the equilibrium $\vec{x} = 0$ is asymptotically stable if and only if $\mathcal{R}e(\lambda) < 0$ for each eigenvalue λ of $D\vec{V}(0,0)$. In other words, the spectrum must lie in the left half-plane of the complex λ plane. This criterion is particularly valuable, considering the extension of the results to non-linear systems. If $\vec{x} = 0$ is asymptotically stable for equation (19), then it will also be asymptotically stable for the original non-linear system (17). Figures Vb and Vc show a schematic phase portrait for a two-dimensional system with two fixed points on the x_1 axis. Linearising about the stable equilibrium at the origin, the resulting 2×2 matrix will have a complex conjugate pair of eigenvalues $(\lambda, \bar{\lambda})$, satisfying $\mathcal{R}e(\lambda) = \mathcal{R}e(\bar{\lambda}) < 0$. The phase portrait for the linearised system

is shown in figure Vb, for arbitrary large initial conditions. In the non-linear phase portrait of figure Vc, $\vec{x} = 0$ is also asymptotically stable, but the neighbourhood $0 < |\vec{x}(0)| < \varepsilon$ of stable initial conditions is not arbitrarily large. In fact it must not intersect the trajectories which are asymptotically drawn to the unstable fixed point on the negative x_1 axis.

The qualitative relation between equations (17) and (19), provided by the property of asymptotic stability, is only applicable when all the eigenvectors are stable, i.e. when E^u and E^c are empty. This, however, does not exhaust the information about the non-linear problem, as the linearised dynamics still remains a qualitatively accurate description of the non-linear one. The following theorem, known as the *Hartman-Grobman* theorem, provides a precise statement of this idea:

Hartman-Grobman Theorem

Let $\vec{x} = 0$ be a hyperbolic equilibrium for equation (17) (i.e. a fixed point with no eigenvalues on the imaginary axis) at some fixed value of μ. Let also ϕ_t and $\tilde{\phi}_t$ denote the flow of (17) and the flow for the corresponding linear system $\dot{\vec{x}} = D\vec{V}(\mu, 0)\, \vec{x}$ respectively. Then there exists a homeomorphism $\Psi : \mathcal{R}^n \to \mathcal{R}^n$, and a neighbourhood U of $\vec{x} = 0$, where

$$\phi_t(\vec{x}) = \Psi^{-1}(\vec{x}) \circ \tilde{\phi}_t(\vec{x}) \circ \Psi(\vec{x}) \tag{20}$$

for all $(\vec{x}, t)$, such that $\vec{x} \in U$ and $\phi_t(\vec{x}) \in U$.

If there are no unstable directions, so that $\Psi(\vec{x})$ belongs to E^s, then $\tilde{\phi}_t(\vec{x}) \circ \Psi(\vec{x}) \to 0$ as $t \to \infty$ for the linear flow, and equation (20) implies that $\phi_t(\vec{x}) \to 0$ as $t \to \infty$ as well. In other words, the theorem implies that any qualitative change in the *local* non-linear dynamics must be reflected in the linear dynamics as well. When E^c is void, the linearised system is qualitatively characterised by the expanding and contracting flows on E^u and E^s, this qualitative structure remaining fixed, unless the equilibrium loses its hyperbolicity. For this loss to occur, the eigenvalues of the stability matrix $D\vec{V}(\mu, 0)$ must shift so as to touch the imaginary axis, which is possible due to the dependence of the system's associated linear stability matrix $D\vec{V}(\mu, 0)$ on μ. As this parameter value changes, it is possible for the eigenvalue $\lambda(\mu)$ to satisfy $\mathcal{R}e(\lambda) = 0$. The system then is said to be *critical* and the corresponding parameter value $\mu = \mu_c$ belongs to the so-called *bifurcation set*.

Loss of hyperbolicity can occur in either of the following ways, distin-

guishable by the appearance of their spectrum at criticality :

- A simple eigenvalue $\lambda_c = 0$.

  This case is referred to with the name *steady-state bifurcation*, appearing in the form of *saddle-node*, *transcritical* or even *pitchfork* bifurcation.

- A simple conjugate pair of eigenvalues $(\lambda, \bar{\lambda})$
  satisfying $\mathcal{R}e(\lambda_c) = \mathcal{R}e(\bar{\lambda}_c) = 0$.

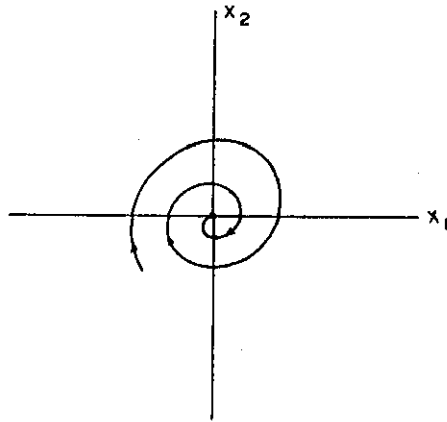 This type of instability is commonly referred to as *Hopf bifurcation*.

Figure Vb.
Asymptotic stability of $\vec{x} = 0$ - The linear case.
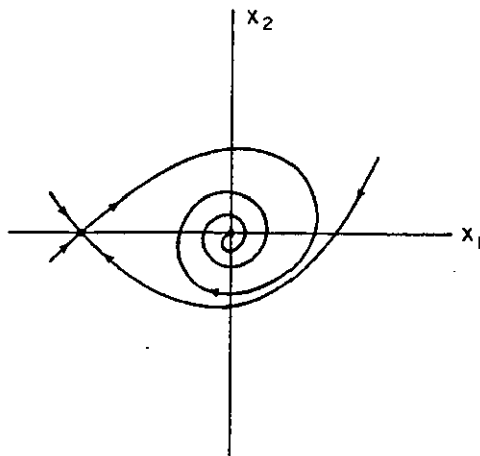
Figure Vc.
Asymptotic stability of $\vec{x} = 0$ -The non-linear case.

IIb. Linearisation in maps

According to J. Crawford [6], the corresponding linear theory for a map follows similar steps : The expansion of equation (17), at $\vec{x} = 0$,

$$\vec{x}_{j+1} = \vec{f}(\mu, 0) + D\vec{f}(\mu, 0)\, \vec{x}_j + \mathcal{O}(|\,\vec{x}\,|^2)\quad,$$

leads to the linearised system

$$\vec{x}_{j+1} = \vec{f}(0,0) + D\vec{f}(0,0)\, \vec{x}_j \tag{21}$$

at $\mu = 0$. Diagonalising the matrix $D\vec{f}(0,0)$ by making the change of coordinates $\vec{x} \to \vec{\tilde{x}}$ as before, the system

$$
\begin{bmatrix} \tilde{x}_1 \\ \tilde{x}_2 \\ . \\ . \\ . \\ \tilde{x}_n \end{bmatrix}_{j+1}
=
\begin{bmatrix} \lambda_1 & 0 & . & . & . & 0 \\ 0 & \lambda_2 & & & & . \\ . & & . & & & . \\ . & & & . & & . \\ . & & & & 0 & \\ 0 & & . & . & 0 & \lambda_n \end{bmatrix}
\begin{bmatrix} \tilde{x}_1 \\ \tilde{x}_2 \\ . \\ . \\ . \\ \tilde{x}_n \end{bmatrix}_{j}
\quad,
$$

is obtained, with solution

$$
\begin{bmatrix} \tilde{x}_1 \\ \tilde{x}_2 \\ . \\ . \\ . \\ \tilde{x}_n \end{bmatrix}_{j}
=
\begin{bmatrix} \lambda_1^j & 0 & . & . & . & 0 \\ 0 & \lambda_2^j & & & & . \\ . & & . & & & . \\ . & & & . & & . \\ . & & & & 0 & \\ 0 & & . & . & 0 & \lambda_n^j \end{bmatrix}
\begin{bmatrix} \tilde{x}_1 \\ \tilde{x}_2 \\ . \\ . \\ . \\ \tilde{x}_n \end{bmatrix}_{0}
\quad.
$$

If $|\,\lambda_i\,| < 1$ then as $j \to \infty$, the $\tilde{x}_i$ component decays exponentially. The case $|\,\lambda_i\,| > 1$ will cause a growth in the $\tilde{x}_i$ component of $\vec{x}$.

For the linearised map of equation (21) the eigenspaces E_λ for the matrix $D\vec{f}(0,0)$ are defined as previously by replacing $D\vec{V}(0,0)$ with $D\vec{f}(0,0)$, and the invariant linear subspaces E^α (where $\alpha = s, c, u$), are now given by replacing $\mathcal{R}e(\lambda)$ by $|\,\lambda\,|$ as follows:

$$E^s \equiv span\{\vec{v}|\ \vec{v} \in E_\lambda \quad and \quad |\,\lambda\,| < 1\}\quad,$$

$$E^u \equiv span\{\vec{v}|\ \vec{v} \in E_\lambda \quad and \quad |\,\lambda\,| > 1\}\quad,$$

$$E^c \equiv span\{\vec{v}|\ \vec{v} \in E_\lambda \quad and \quad |\,\lambda\,| = 1\}\quad.$$

Similarly as before, $\mathcal{R}^n = E^s \oplus E^c \oplus E^u$, and the asymptotic dynamics are the same for the stable and unstable subspaces, for $j \to \infty$ and $j \to -\infty$ respectively. For the linear dynamics of equation (21) the equilibrium $\vec{x} = 0$ will be asymptotically stable if and only if the spectrum of $D\vec{f}(0,0)$ lies within the unit circle in the complex λ plane, i.e. $\mid \lambda_i \mid < 1$ for each eigenvalue. It can be shown that if $\vec{x} = 0$ is asympotically stable for equation (21) then the same conclusion holds for the non-linear dynamics of equation (17) as well.

As in the case of linear flows, a fixed point is called hyperbolic if the centre subspace E^c is empty. The Hartman-Grobman theorem relates the linearised dynamics to the local non-linear dynamics : If at $(\vec{x} = 0, \mu = 0)$ there is a hyperbolic fixed point, there exists a homeomorphism Ψ and a local neighbourhood U of $\vec{x} = 0$ where

$$\vec{f}(0, \vec{x}) = \Psi^{-1}(\vec{x}) \left(D\vec{f}(0,0) \; \Psi(\vec{x}) \right)$$

such that $\vec{x} \in U$ and $\vec{f}(0, \vec{x}) \in U$. If $\vec{x} = 0$ is a hyperbolic fixed point for $\vec{f}(\mu, \vec{x})$ at $\mu = 0$, then as μ is varied around $\mu = 0$ the equilibrium will be shifted with regard to its location, but it will nevertheless persist. The eigenvalues of $D\vec{f}(\mu, 0)$ will be functions of μ and any variation around $\mu = 0$ will cause them to move in the complex plane. When an eigenvalue reaches the unit circle, the fixed point loses its hyperbolicity, and it is possible for a bifurcation to occur.

In the case where the condition $\mid \lambda_i \mid \neq 1$ fails the following three possibilities can be classified:

- A simple real eigenvalue at $\lambda_c = 1$.

  This type of instability is similar to the $\lambda_c = 0$ case for flows. It is referred to as *steady-state* bifurcation for maps. More detailed study reveals examples of *saddle-node, transcritical* and *pitchfork* bifurcation as well.

- A simple conjugate pair of eigenvalues $(\lambda, \bar{\lambda})$ satisfying $\lambda_c = e^{i2\pi\theta}$.

  This case is referred to as *Hopf* bifurcation for maps.

- A simple real eigenvalue at $\lambda_c = -1$.

  This case doesn't have any direct analog in the theory of flows. Its related instability is generally called *period-doubling* bifurcation.

IIc. The centre manifold reduction

According to J. Guckenheimer [17], denoting $E^h = E^s \oplus E^u$, there exists $\vec{\Psi} \in C^k(E^c; E^h)$ such that

$$\vec{\Psi}(0) = 0, \qquad D\vec{\Psi}(0) = 0 \quad ,$$

and a neighbourhood U of $\vec{x} = 0$, such that the manifold

$$M_0 \equiv \{\, \vec{x} + \vec{\Psi}(\vec{x})|\ \vec{x} \in E^c \,\}, \qquad \vec{x} \in \mathcal{R}^n$$

- is locally invariant in the sense that, if $\vec{x}(0) \in M_0 \cap U$ and $\vec{x}(t) \in U$, then it is also $\vec{x}(t) \in M_0$, $\forall t > 0$.

- contains all solutions of (17) staying in U, i.e. if $\vec{x}(0) \in U$ and $\vec{x}(t) \in U$, then in the case where neither E^s nor E^u is void, also $\vec{x}(0) \in M_0$

  and finally

- is locally attractive when E^u is void, which means that all solutions $\vec{x}(t)$, staying in U for all $t > 0$, tend exponentially to some solution $\vec{\bar{x}}(t)$ on M_0.

J. Guckenheimer (see [17]) describes the manifold M_0 as a C^k-manifold of $\mathcal{R}^n$ parametrised by $\vec{x} \in E^c$. Hence it has the same dimension as E^c, passes through $\vec{x} = 0$ and it is tangent to E^c at $\vec{x} = 0$. M_0 is said to be the *centre manifold* of (17) at $\vec{x} = 0$.

Letting Π be the projection from $\mathcal{R}^n$ on to E^c, and defining

$$\vec{y}(t) \equiv \Pi\vec{x}(t)$$

so that $\vec{y}(0) = \Pi\vec{x}(0)$,

$$\vec{x}(t) = \vec{y}(t) + \vec{\Psi}\left(\vec{y}(t)\right) \quad .$$

Equation (17) now takes the form

$$\dot{\vec{y}}(t) = \Pi F\left(\vec{y}(t) + \vec{\Psi}\left(\vec{y}(t)\right)\right) \equiv \vec{V}(\mu, \vec{y}), \qquad \vec{y} \in E^c \quad .$$

The above equation is the so-called *reduced equation* of (17).

IId. The technique

The following four-step technique is described in more detail in [6], though a similar technique for the study of stability of equilibria can be found in [3]. Suppose that an asymptotically stable equilibrium is perturbed by varying an external parameter μ, and at a critical value $\mu = \mu_c$ the equilibrium loses its hyperbolicity ($\mathcal{R}e(\lambda) = 0$ in the case of flows, $|\lambda| = 1$ for maps). It is interesting to examine what happens to the system as μ is varied about μ_c.

Our study follows the following four-step technique:

- **(1) Reduction**

  Identify the neutral mode (or modes) of the system at $\mu = \mu_c$ and restrict the dynamical system to the appropriate centre manifold.

  The dimension of the problem is this way reduced, without any loss of essential information concerning the bifurcation.

- **(2) Normalisation**

  Apply near-identity coordinate changes.

  The dynamical system is thus put into a simpler form, yielding the normal form for the bifurcation.

- **(3) Unfolding**

  Introduce small terms into the normal form.

  This is done in order to describe the effects of varying μ about μ_c.

- **(4) Truncation**

  Truncate some of the system's main equation higher-order terms.

  The resulting system can be more easily understood, allowing the effects of restoring the higher-order terms to be studied later, though in the case of sufficiently complicated bifurcations these effects can be significant and highly non-trivial.

IIe. The implicit function theorem

The following theorem, known as the *implicit function theorem*, provides the necessary information for an equilibrium of a flow or a map, as μ varies. The theorem can also be found in [3, 6, 17].

Implicit Function theorem

Let $\vec{G}(\mu, \vec{x})$ be a C^1 function on $\mathcal{R} \times \mathcal{R}^n$,

$$\vec{G}: \ \mathcal{R} \times \mathcal{R}^n \to \mathcal{R}^n \quad,$$

such that

$$\vec{G}(0,0) = 0$$

and

$$det[D\vec{G}(0,0)] \neq 0 \quad.$$

There exists a unique differentiable function $\vec{X}(\mu)$ defined on a neighbourhood $M \subset \mathcal{R}$ of $\mu = 0$,

$$\vec{X}: \ M \to \mathcal{R}^n \quad,$$

such that $\vec{X}(0) = 0$ and

$$\vec{G}(\mu, \vec{X}(\mu)) = 0, \qquad \mu \in M \quad.$$

According to the above theorem, given the function $\vec{G}(\mu, \vec{x})$ the set of $(\mu, \vec{x})$ satisfying $\vec{G}(\mu, \vec{x}) = 0$ is assumed to contain at least one point $(0,0)$. If in addition the matrix

$$\left(D\vec{G}(0,0)\right)_{ij} \equiv \frac{\partial G_i}{\partial x_j}(0,0) \qquad i,j = 1, \cdots, n$$

has a non-zero determinant, than the equation $\vec{G}(\mu, \vec{X}(\mu)) = 0$ can be solved uniquely for $\vec{x}$ as a function of μ, at least for values of μ sufficiently near $\mu = 0$. In the theory's terminology, the zero set of $\vec{G}(\mu, \vec{x})$ consists of a single *branch* near $(\mu, \vec{x}) = (0,0)$, as shown in figure Vd.
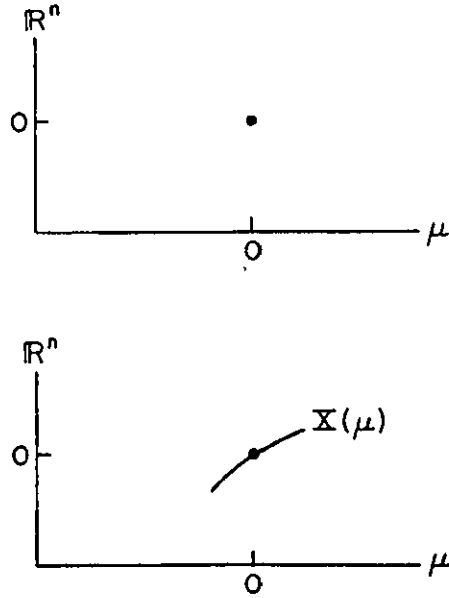
Figure Vd. A unique solution branch from the implicit function theorem. Given $\vec{G}(0,0) = 0$ and $det[D\vec{G}(0,0)] \neq 0$ at a point (a), the local structure of the solution set for $\vec{G}(\mu,\vec{x}) = 0$ is a single branch (b).

In order to apply the above theorem to flows, after choosing $\vec{G}(\mu,\vec{x}) = \vec{V}(\mu,\vec{x})$ the relation

$$det[D\vec{G}(0,0)] = det[D\vec{V}(0,0)]$$

implies that the above determinant will be non-zero if and only if $\lambda = 0$ is not an eigenvalue for $D\vec{V}(0,0)$. As long as this holds the equilibrium solution cannot be destroyed and the solution must in fact persist and lie on a local branch of solutions $\vec{X}(\mu)$, determined by the implicit function theorem.

Two conclusions can be drawn from the above :

- In steady-state bifurcation the condition $det[D\vec{V}(0,0)] \neq 0$ fails, since by definition there is always an eigenvalue at zero.

  This implies that in general one cannot expect a unique branch of equilibria through $(\mu,\vec{x}) = (0,0)$ for a fixed point at criticality.

- In the case of Hopf bifurcation the number of equilibrium solutions persist, since the only eigenvalues of $D\vec{V}(0,0)$ on the imaginary axis form a conjugate pair.

52

In the case of maps, J. Crawford in [6] suggested that, choosing

$$\vec{G}(\mu, \vec{x}) = \vec{f}(\mu, \vec{x}) - \vec{x} \quad,$$

so that

$$\vec{G}(0, 0) = 0$$

and

$$D\vec{G}(0, 0) = D\vec{f}(0, 0) - I \quad,$$

where I is the identity matrix on $\mathcal{R}^n$, then, if $\vec{G}(\mu, \vec{x}) = 0$, $\vec{x} = 0$ is a fixed point for the map at parameter value μ. For the solution $(\mu, \vec{x}) = (0, 0)$ the determinant of $\left(D\vec{f}(0, 0) - I\right)$ will be non-zero if and only if the linear stability matrix $D\vec{f}(0, 0)$ does not have an eigenvalue at $\lambda = +1$. This provided, the implicit function theorem implies that $(\mu, \vec{x}) = (0, 0)$ lies on an isolated branch of equilibrium solutions.

As before,

- in steady-state bifurcation, $\lambda = +1$.

- neither period-doubling nor Hopf bifurcation can alter the number of equilibrium solutions.

III. STEADY-STATE BIFURCATIONS

IIIa. General features

Considering flows, in the case of steady-state bifurcation there is a simple eigenvalue at zero and the centre manifold reduction yields a one-dimensional system of the form

$$\dot{x} = V(\mu, x) \quad , \qquad x \in \mathcal{R}, \qquad \mu \in \mathcal{R}, \tag{22}$$

arising at criticality and satisfying

$$V(0,0) = 0 \quad ,$$

and

$$\frac{\partial V}{\partial x}(0,0) = 0 \quad .$$

J. Crawford in his work in [6] suggests that the study of bifurcations near equilibria should start by exploring what happens in equation (22) as (μ, x) gets close to $(0,0)$. This can be done by expanding equation (22) at $(\mu, x) = (0,0)$ one gets

$$\dot{x} = \frac{\partial V}{\partial \mu}(0,0)\mu + \frac{\partial^2 V}{\partial x^2}(0,0)\frac{x^2}{2} + \frac{\partial^2 V}{\partial x \partial \mu}(0,0)\mu x +$$

$$+\frac{\partial^2 V}{\partial \mu^2}(0,0)\frac{\mu^2}{2} + \frac{\partial^3 V}{\partial x^3}(0,0)\frac{x^3}{3!} + \cdots \tag{23}$$

In maps there is a simple eigenvalue at $\lambda = +1$ and the normal form will be

$$x_{j+1} = f(\mu, x_j) \qquad \mu \in \mathcal{R}, \ x \in \mathcal{R}$$

where $j = 0, 1, 2, \cdots$,

$$f(0,0) = 0 \quad ,$$

and

$$\frac{\partial f}{\partial x}(0,0) = +1 \quad .$$

Denoting $V(\mu, x) \equiv f(\mu, x_j) - x$, there follows

$$V(0,0) = 0$$

54

and

$$\frac{\partial V}{\partial x}(0,0) = 0 \quad .$$

The resulting bifurcation forms for maps can be worked out exactly as in the case of flows. The only difference is the extra case of period-doubling bifurcation.

In the sub-sections IIIb-IIId that follow, the normal forms that J. Guckenheimer [17] gives for the study of each of the bifurcation types, have been analytically worked out from equation (23), applying near-identity coordinate changes. This is in accordance to the study of J. Crawford in [6].

IIIb. Saddle-node bifurcation

In the case where

$$\frac{\partial V}{\partial \mu}(0,0) \neq 0$$

and

$$\frac{\partial^2 V}{\partial x^2}(0,0) \neq 0 \quad ,$$

equation (23) can be rewritten as

$$\dot{x} = \frac{\partial V}{\partial \mu}(0,0)\mu\left[1 + \mathcal{O}(\mu, x)\right] + \frac{\partial^2 V}{\partial x^2}(0,0)\frac{x^2}{2}\left[1 + \mathcal{O}(\mu, x)\right] \quad ,$$

where $\mathcal{O}(\mu, x)$ indicates terms that are first order at least in μ or x, negligible near $(\mu, x) = (0, 0)$. Defining rescaled variables $(\tilde{\mu}, \tilde{x})$ so that

$$\tilde{\mu} = \frac{1}{2}\,\mu\,\left|\frac{\partial V}{\partial \mu}(0,0)\frac{\partial^2 V}{\partial x^2}(0,0)\right| \quad ,$$

$$\tilde{x} = \frac{1}{2}\,x\,\left|\frac{\partial^2 V}{\partial x^2}(0,0)\right| \quad ,$$

finally the normal form

$$\dot{\tilde{x}} = \epsilon_1\tilde{\mu} + \epsilon_2\tilde{x}^2 \equiv \tilde{V}(\tilde{\mu}, \tilde{x}) \quad , \tag{24}$$

is obtained, where

$$\epsilon_1 \equiv sgn\left[\frac{\partial V}{\partial \mu}(0,0)\right] \quad ,$$

and

$$\epsilon_2 \equiv sgn\left[\frac{\partial^2 V}{\partial x^2}(0,0)\right] \quad .$$

Near equilibrium $(\tilde{\mu} = 0, \tilde{x} = 0)$ and assuming that $\epsilon_1 = \epsilon_2 = +1$, equation (24) takes the form

$$\tilde{\mu} + \tilde{x}^2 = 0 \quad ,$$

in fact describing a parabola in the $(\tilde{\mu} = 0, \tilde{x} = 0)$ plane, as shown in figure Ve. At a fixed value of $\tilde{\mu} > 0$ there are two equilibria $\tilde{x}_\pm(\tilde{\mu}) = \pm\sqrt{-\tilde{\mu}}$, coinciding as $\tilde{\mu}$ increases to criticality. The upper branch $\tilde{x}_+(\tilde{\mu})$ is unstable, whereas the lower branch $\tilde{x}_-(\tilde{\mu})$ is asymptotically stable. This

can be checked by letting $\tilde{y}_\pm \equiv \tilde{x}_\pm - \tilde{x}$ and linearising equation (23) about $\tilde{x}_\pm(\tilde{\mu})$:

$$\dot{\tilde{y}}_\pm = \frac{\partial \tilde{V}}{\partial \tilde{x}}(\tilde{\mu}, \tilde{x}_\pm)\, \tilde{y}_\pm = [2\, \tilde{x}_\pm(\tilde{\mu})]\, \tilde{y}_\pm \quad .$$

The eigenvalue $[2\tilde{x}_\pm(\tilde{\mu})]$ is positive (unstable) for $\tilde{x}_+$ and negative (unstable) for $\tilde{x}_-$. It is worth noticing that for $\tilde{\mu} < 0$ there are two equilibria, but none in the case where $\tilde{\mu} > 0$. This is consistent with the fact that the determinant of $DV(0,0)$ becomes zero, and the implicit function theorem fails to guarantee a unique branch of equilibria passing through $(0,0)$. The saddle-node bifurcation described above is shown in figure Ve-a.

The three other cases, $[\epsilon_1 = \epsilon_2 = -1]$, $[-\epsilon_1 = \epsilon_2 = +1]$ and $[\epsilon_1 = -\epsilon_2 = +1]$, together with the corresponding bifurcation diagrams, can be worked out in a similar way.

Dealing with maps, it is again assumed that

$$\frac{\partial V}{\partial \mu}(0,0) \neq 0$$

and

$$\frac{\partial^2 V}{\partial x^2}(0,0) \neq 0 \quad .$$

The resulting equation, after rescaling the variables, will be

$$\tilde{x}_{j+1} = \epsilon_1 \tilde{\mu} + \tilde{x}_j + \epsilon_2 \tilde{x}_j^2 \equiv \tilde{f}(\tilde{\mu}, \tilde{x}_j) \quad , \tag{25}$$

with

$$\epsilon_1 \equiv sgn\left[\frac{\partial f}{\partial \mu}(0,0)\right] \quad ,$$

and

$$\epsilon_2 \equiv sgn\left[\frac{\partial^2 f}{\partial x^2}(0,0)\right] \quad .$$

There are two fixed points, $\tilde{x}_\pm(\tilde{\mu}) = \pm\sqrt{-\tilde{\mu}}$ with corresponding linear eigenvalues

$$\frac{\partial \tilde{f}}{\partial \tilde{x}}(\tilde{\mu}, \tilde{x}_\pm) = 1 + 2\,\epsilon_2\,\tilde{x}_\pm(\tilde{\mu}) \quad .$$

The resulting equilibrium is stable, if $\epsilon_2 \tilde{x}_\pm(\tilde{\mu})$ is negative, and unstable if it is positive. The bifurcation diagrams turn out to be the same as those related to flows (figure Ve).
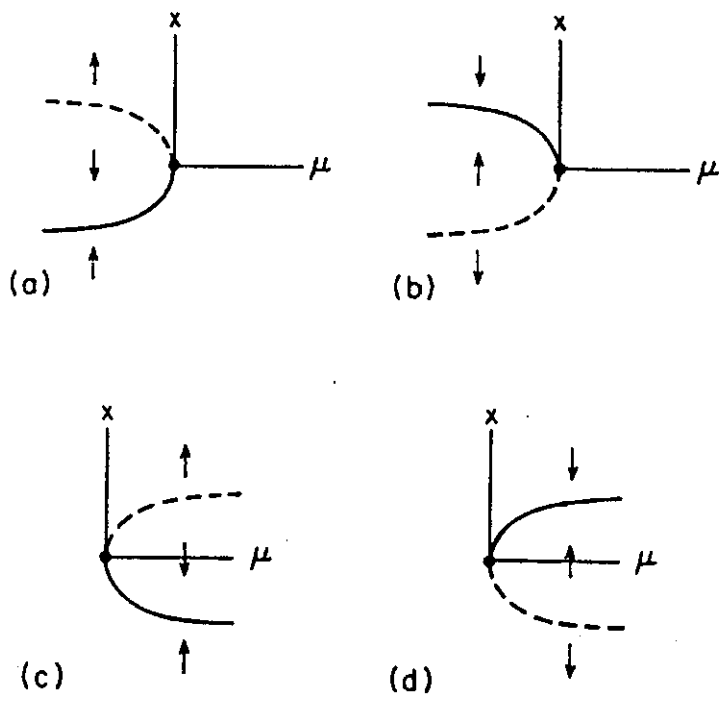
Figure Ve.
Saddle-node bifurcation.
(a) $\epsilon_1 = \epsilon_2 = +1$, (b) $\epsilon_1 = \epsilon_2 = -1$, (c) $-\epsilon_1 = \epsilon_2 = +1$,
(d) $\epsilon_1 = -\epsilon_2 = +1$.
Solid branches denote stable equilibrium; dashed branches unstable.

58

IIIc. Transcritical bifurcation

It is possible for an asymptotically stable equilibrium to lose stability through a steady-state bifurcation, but for the equilibrium itself to persist. Denoting in this case the equilibrium by $X(\mu)$, such that $X(0) = 0$, there will be

$$V(\mu, X(\mu)) = 0, \qquad \mu \in \mathcal{R} \quad,$$

while it is possible for $V(\mu, x)$ to be appropriately redefined by making the μ-dependent change of variables

$$x = X(\mu) + \tilde{x} \quad.$$

Setting $X(\mu) = 0$ and dropping the tildes,

$$V(\mu, 0) = 0 \quad.$$

The above relation implies

$$\frac{\partial^n V}{\partial \mu^n}(0,0) = 0, \qquad n = 1, 2, \cdots$$

and, taking the Taylor expansion around $(\mu, x) = (0,0)$,

$$\dot{x} = \frac{\partial^2 V}{\partial x \partial \mu}(0,0)\mu x + \frac{\partial^2 V}{\partial x^2}(0,0)\frac{x^2}{2} + \frac{\partial^3 V}{\partial x^3}(0,0)\frac{x^3}{3!} + \cdots \quad.$$

Assuming that

$$\frac{\partial^2 V}{\partial x \partial \mu}(0,0) \neq 0$$

and

$$\frac{\partial^2 V}{\partial x^2}(0,0) \neq 0 \quad,$$

the variables are rescaled exactly the same way as in the saddle-node case, yielding the normal form

$$\dot{\tilde{x}} = \tilde{x}\left(\epsilon_1 \tilde{\mu} + \epsilon_2 \tilde{x}\right) \quad, \tag{26}$$

where

$$\epsilon_1 \equiv sgn\left[\frac{\partial^2 V}{\partial x \partial \mu}(0,0)\right] \quad,$$

and

$$\epsilon_2 \equiv sgn\left[\frac{\partial^2 V}{\partial x^2}(0,0)\right] \quad.$$

The point $x = 0$ is now an equilibrium point for all $\tilde{\mu}$, while it is worth noticing that at $\tilde{\mu} = 0$ the eigenvalue $\epsilon_1 \tilde{\mu}$ becomes zero. The equilibrium $x = 0$ is stable for $sgn\,(\epsilon_1 \mu) = -1$ and unstable when $sgn\,(\epsilon_1 \mu) = +1$.

There is a second branch of equilibria arising from the second factor of the right-hand side of equation (26),

$$\tilde{x}_b(\tilde{\mu}) = - \left[\frac{\epsilon_1}{\epsilon_2}\right] \tilde{\mu}$$

with a type of stability found by linearising:
The assumption $y = \tilde{x}_b - \tilde{x}$ reveals $\dot{y} = (-\epsilon_1 \tilde{\mu})\, y$.

The equilibria $\tilde{x} = 0$ and $\tilde{x} = \tilde{x}_b(\tilde{\mu})$ have opposite stabilities. They collide, however, at $\tilde{\mu} = 0$, and their stabilities are exchanged. The final form of the resulting bifurcation diagram depends on the values of ϵ_1 and ϵ_2.

The four possibilities for equilibrium are shown in Figure Vf.

In the case of maps, there too holds

$$\frac{\partial^2 V}{\partial x^2}(0,0) \neq 0 \quad,$$

and

$$\frac{\partial^2 V}{\partial x \partial \mu}(0,0) \neq 0 \quad,$$

while as previously one can obtain

$$\tilde{x}_{j+1} = \tilde{x}_j \left(1 + \epsilon_1 \tilde{\mu} + \epsilon_2 \tilde{x}_j\right) \equiv \tilde{f}(\tilde{\mu}, \tilde{x}_j) \quad. \tag{27}$$

The bifurcation diagrams are that of figure Vf, as well as the stability assignments, since the linear eigenvalues for the fixed points $\tilde{x} = 0$ and $\tilde{x} = \tilde{x}_b$ are $(1 + \epsilon_1 \tilde{\mu})$ and $(1 - \epsilon_1 \tilde{\mu})$ respectively. At $\tilde{\mu} = 0$ the two branches merge and their stability is exchanged.
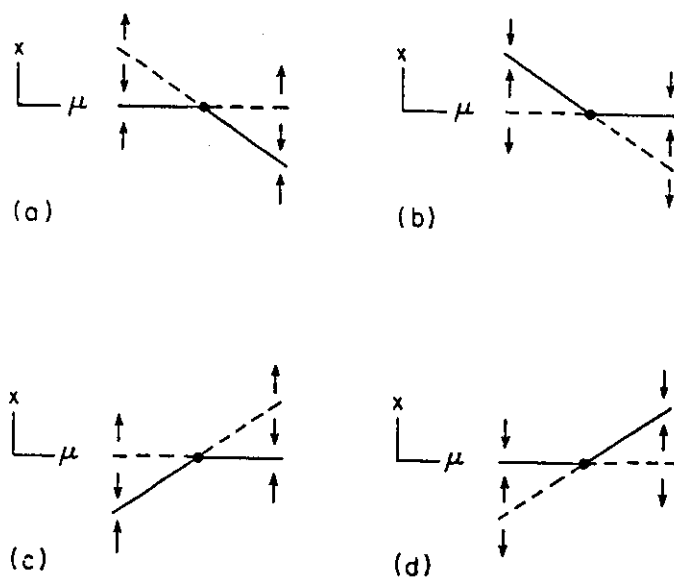
Figure Vf.
Transcritical bifurcation.
(a) $\epsilon_1 = \epsilon_2 = +1$, (b) $\epsilon_1 = \epsilon_2 = -1$, (c) $-\epsilon_1 = \epsilon_2 = +1$,
(d) $\epsilon_1 = -\epsilon_2 = +1$.
Solid branches denote stable equilibrium; dashed branches unstable.

IIId. Pitchfork bifurcation

This version of steady-state bifurcation arises when

$$\frac{\partial^2 V}{\partial x \partial \mu}(0,0) \neq 0 \quad ,$$

and

$$\frac{\partial^3 V}{\partial x^3}(0,0) \neq 0 \quad .$$

A natural context for these assumptions is that $V(\mu, x)$ has a reflection symmetry,

$$V(\mu, x) = -V(\mu, -x) \quad ,$$

which obviously implies $V(\mu, 0) = 0$.

The corresponding Taylor expansion now takes the form

$$\dot{x} = \frac{\partial^2 V}{\partial x \partial \mu}(0,0)\mu x \left[1 + \mathcal{O}(\mu, x)\right] + \frac{\partial^3 V}{\partial x^3}(0,0)\frac{x^3}{3!}\left[1 + \mathcal{O}(\mu, x)\right] \quad .$$

As done previously, by truncating the higher order terms and rescaling variables one gets

$$\dot{\tilde{x}} = \tilde{x}\left[\epsilon_1 \tilde{\mu} + \epsilon_2 \tilde{x}^2\right] \quad , \tag{28}$$

where

$$\epsilon_1 \equiv sgn\left[\frac{\partial^2 V}{\partial x \partial \mu}(0,0)\right] \quad ,$$

and

$$\epsilon_2 \equiv sgn\left[\frac{\partial^3 V}{\partial x^3}(0,0)\right] \quad .$$

There are now two branches of equilibria appearing, namely the

$$\tilde{x}_\pm(\tilde{\mu}) = \pm\sqrt{-\left(\epsilon_1/\epsilon_2\right)\tilde{\mu}} \quad ,$$

existing only for $sgn\left(\epsilon_1/\epsilon_2\tilde{\mu}\right) = -1$. The stability of the solutions can be worked out as before, and the four possibilities are illustrated in figure Vg.

In the case of maps, assuming that

$$\frac{\partial^3 V}{\partial x^3}(0,0) \neq 0 \quad ,$$

and

$$\frac{\partial^2 V}{\partial x \partial \mu}(0,0) \neq 0 \quad ,$$

we obtain, after the appropriate rescaling of variables

$$\tilde{x}_{j+1} = \tilde{x}_j \left(1 + \epsilon_1 \tilde{\mu} + \epsilon_2 \tilde{x}_j^2\right) \equiv \tilde{f}(\tilde{\mu}, \tilde{x}_j) \quad , \tag{29}$$

with corresponding bifurcation diagrams those shown in figure Vg below:
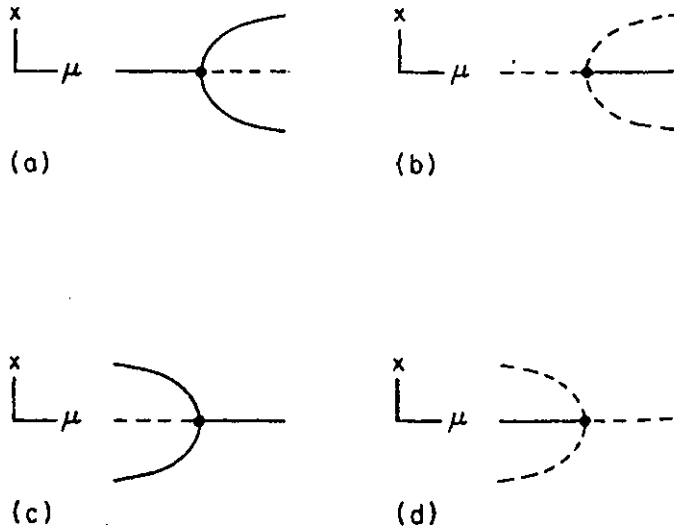

Figure Vg.
Pitchfork bifurcation.
(a) $\epsilon_1 = -\epsilon_2 = +1$, (b) $-\epsilon_1 = \epsilon_2 = +1$, (c) $\epsilon_1 = \epsilon_2 = -1$,
(d) $\epsilon_1 = \epsilon_2 = +1$.
Solid branches denote stable equilibrium; dashed branches unstable.

IIIe. Perturbations in the steady-state bifurcation

J. Crawford in [6] introduces the concept of perturbations in the steady-state bifurcation, as follows: Perturbations occurring in the transcritical or pitchfork bifurcations can restore the so-called generic behaviour of the system, which is the saddle-node bifurcation: Suppose that $V(\mu, x)$ describes a transcritical or pitchfork bifurcation at $(\mu, x) = (0, 0)$. By including a small term $V_1(\mu, x)$ in the dynamics, $V(\mu, x)$ can be perturbed is such a way that

$$\dot{x} = V(\mu, x) + \epsilon\, V_1(\mu, x) \quad,$$

where $0 \leq \epsilon \ll 1$. The perturbation V_1 may be chosen arbitrarily, in the sense that there is no need for special assumptions.

For transcritical bifurcation and in the case where $\epsilon \neq 0$, the related bifurcation diagram can be modified in two possible ways (see figure Vh(a)), the first one containing two saddle-node bifurcations and the other one no bifurcations at all. In the case of pitchfork bifurcation there are four possibilities, as shown in figure Vh(b). By closer examination of the perturbed diagrams one can find that *hysteresis* in the bifurcations of the perturbed pitchfork can appear: When $\epsilon = 0$ the outer branches of the pitchfork meet the middle one with an angle of 90°. Small perturbations in the dynamics can slightly change this angle, as shown in figure Vh(b), allowing hysteresis to occur.
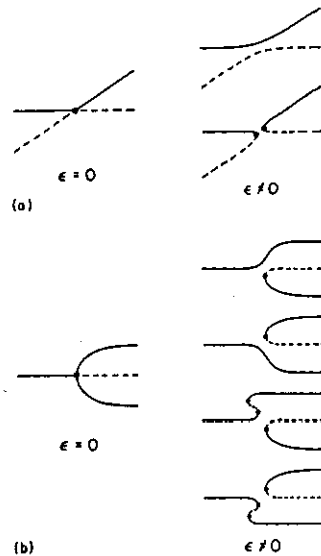

Figure Vh. Perturbing non-generic diagrams.
(a) Transcritical bifurcation, (b) Pitchfork bifurcation.

IIIf. Period-doubling bifurcation

This type of bifurcation arises only when dealing with maps. The following study, including the key observation that it is actually the twice-iterated map of $f(\mu, x)$ that undergoes a bifurcation, closelly follows the work of j. Crawford in [6].

There is

$$x_{j+1} = f(\mu, x_j), \qquad \mu \in \mathcal{R}, \; x \in \mathcal{R} \quad , \tag{30}$$

$$f(\mu, 0) = 0 \quad ,$$

$$\frac{\partial f}{\partial x}(0, 0) = -1 \quad ,$$

and the one-dimensional normal form will have a reflection symmetry

$$f(\mu, -x) = -f(\mu, x) \quad .$$

In the relations above a proper coordinate shift is assumed in order to place the persisting equilibrium branch at the origin.

At the fixed point $x = 0$ the Taylor expansion of $f(\mu, x)$ takes the form

$$f(\mu, x) = \lambda(\mu)x + \alpha_1(\mu)x^3 + \alpha_2(\mu)x^5 + \mathcal{O}(x^7) \quad ,$$

where $\lambda(0) = -1$.

It is worth noticing that the *twice-iterated* map

$$f^2(\mu, x) \equiv f\left(\mu, f(\mu, x)\right)$$

is undergoing a steady-state bifurcation, in fact a pitchfork-type one because of the reflection symmetry. Taking thus $V(\mu, x) = f^2(\mu, x) - x$ there will be

$$\frac{\partial V}{\partial \mu}(0, 0) = \frac{\partial f}{\partial \mu}(0, 0)\left[1 + \frac{\partial f}{\partial x}(0, 0)\right] = 0 \quad ,$$

$$\frac{\partial^2 V}{\partial x^2}(0, 0) = \frac{\partial^2 f}{\partial x^2}(0, 0)\frac{\partial f}{\partial x}(0, 0)\left[1 + \frac{\partial f}{\partial x}(0, 0)\right] = 0 \quad ,$$

$$\frac{\partial^2 V}{\partial x \partial \mu}(0, 0) = 2\,\frac{\partial f}{\partial x}(0, 0)\frac{\partial^2 f}{\partial x \partial \mu}(0, 0) = -2\,\frac{d\lambda}{d\mu}(0)$$

and

$$\frac{\partial^3 V}{\partial x^3}(0, 0) = \frac{\partial f}{\partial x}(0, 0)\frac{\partial^3 f}{\partial x^3}(0, 0)\left[1 + \left(\frac{\partial f}{\partial x}(0, 0)\right)^2\right] = -12\,\alpha_1(0) \quad .$$

Is it easy to see that for a pitchfork-like bifurcation to occur the following two relations must be assumed to hold:

$$\frac{d\lambda}{d\mu}(0) \neq 0$$

and

$$\alpha_1(0) \neq 0 \quad .$$

After rescaling,

$$\tilde{x}_{j+1} = \tilde{x}_j \left(1 + \epsilon_1\tilde{\mu} + \epsilon_2\tilde{x}_j^2\right) \equiv \tilde{f}(\tilde{\mu}, \tilde{x}_j) \quad , \tag{31}$$

where

$$\epsilon_1 \equiv sgn\left[-\frac{d\lambda}{d\mu}(0)\right] \quad ,$$

$$\epsilon_2 \equiv sgn\left[-\alpha_1(0)\right] \quad ,$$

and the related bifurcation diagrams are shown in figure Vg.

As before, there is loss of stability at $\mu = 0$, though the $\tilde{x}_\pm(\tilde{\mu})$ branches of the pitchfork for $f^2(\mu, x)$ cannot be fixed points for $f(\mu, x)$ as well, as it is guaranteed by the implicit function theorem that $x = 0$ is the unique branch through $(\mu, x) = (0, 0)$. Denoting $\tilde{x}_\pm$ as $x_\pm$ in the original variables of equation (30), there must be

$$x_- = f(\mu, x_+) \quad ,$$

and

$$x_+ = f(\mu, x_-) \quad ,$$

in other words $f(\mu, x)$ is interchanging x_+ and x_- , and the branch $(\tilde{x}_+, \tilde{x}_-)$ is therefore representing a new bifurcation.

IV. HOPF BIFURCATION

IVa. Flows

Hopf bifurcation is a phenomenon richer than steady-state bifurcation in the sense that is can lead to a time-dependent non-linear behaviour. This is the case where the eigenvalues of the stability matrix DV form a complex conjugate pair $\lambda_R(\mu) \pm i\lambda_I(\mu)$, where the relations

$$\lambda_R(0) = 0 \quad ,$$

$$\lambda_I(0) \neq 0 \quad ,$$

and

$$\frac{d\lambda_R(\mu)}{d\mu} > 0 \quad ,$$

express the fact that the conjugate pair crosses the imaginary axis at $\mu = 0$ in a non-degenerate way.

In J. Crawford's work in [6], Hopf bifurcation is described in detail, leading to the following conclusions: The normal form is two-dimensional and it is convenient to express the Taylor expansion in terms of polar coordinates (ρ, θ) as follows,

$$\dot{\rho} = \rho \left[\lambda_R(\mu) + \sum_{j=1}^{\infty} \alpha_j(\mu)\rho^{2j} \right] = \lambda_R \, \rho + \alpha_1 \, \rho^3 + \mathcal{O}(\rho^5) \quad ,$$

and

$$\dot{\theta} = \lambda_I(\mu) + \sum_{j=1}^{\infty} b_j(\mu)\rho^{2j} \quad .$$

A characteristic feature of the above equations is the absence of θ in the right-hand side, arising from the fact that the dynamics of the normal form is invariant with respect to the group of phase rotations.

Assuming that at $\mu = 0$ the cubic coefficient does not vanish, i.e.

$$\alpha_1 (0) \neq 0 \quad ,$$

and it is actually its sign that determines the solutions to $d\rho/dt = 0$ near $\rho = 0$:

Consider the case where $\alpha_1 (0) < 0$. The radial equilibria will be

$$\rho \left[\lambda_R(\mu) + \alpha_1(\mu)\rho^2 \right] \approx 0$$

67

and there are two branches of equilibria, $\rho = 0$ and $\rho_H(\mu) \approx \sqrt{-\lambda_R/\alpha_1}$, as can be shown in figure Vi, the second existing only in the case $\lambda_R(\mu) > 0$. The result is in fact a periodic orbit with amplitude $\rho_H(\mu)$ and frequency

$$[\lambda_I]_H(\mu) = \lambda_I(\mu) + \sum_{j=1}^{\infty} b_j(\mu)\rho_H^{2j} \quad ,$$

which by linearising about $\rho = \rho_H$ and determining the linear eigenvalue, can be proven to be asymptotically stable. The bifurcation of ρ_H is called *supercritical*, due to the fact that the new branch of solutions is found to be in the direction of increasing μ, above the threshold for instability of the equilibrium.

Similarly the case $\alpha_1(0) > 0$ can be analysed. Now the solution ρ_H is found only for $\lambda_R(\mu) < 0$ or $\mu < 0$, and the branch of periodic solutions in unstable (see figure Vj). The bifurcation in this case is said to be *subcritical*.
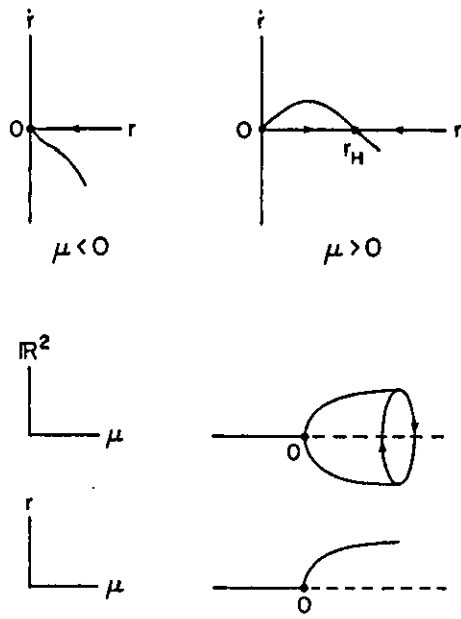
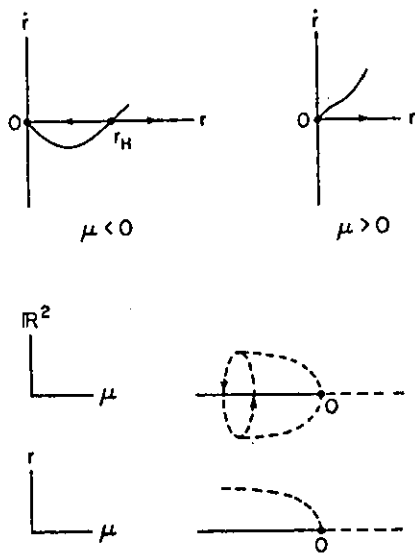Figure Vi.
Hopf Bifurcation, $\alpha_1(0) < 0$.

Figure Vj.
Hopf Bifurcation, $\alpha_1(0) > 0$.

IVb. Maps

The normal form here is again two-dimensional, (the following study closely follows the study in [6]) and the eigenvalues form a simple complex conjugate pair at $|\lambda| = 1$. They can be denoted in the form

$$\lambda(\mu) = [\, 1 + \alpha(\mu)\,]\, e^{i2\pi\phi(1+b(\mu)\,)} \quad,$$

where

$$0 < \phi < \frac{1}{2} \quad,$$

$$\alpha(0) = b(0) = 0 \quad,$$

and

$$\frac{d\alpha(0)}{d\mu} > 0 \quad.$$

If the eigenvalue at criticality, $\lambda(0) = e^{i2\pi\phi}$, satisfies the so-called *non-resonance* conditions

$$[\,\lambda(0)\,]^k \neq 1 \qquad (32)$$

for $k = 3, 4$, then in polar variables (ρ, θ) the normal form of the bifurcation will be

$$\rho_{j+1} = [1 + \alpha(\mu)]\,[1 + \alpha_1(\mu)\rho_j^2 + \mathcal{O}(\rho_j^4)\,]\,\rho_j \quad, \qquad (33)$$

and

$$\theta_{j+1} = \theta_j + 2\pi\phi\,[1 + b(\mu)] + b_1(\mu)\rho_j^2 + \mathcal{O}(\rho_j^4) \quad. \qquad (34)$$

The right-hand side of the above equations is independent of θ, in analogy to the phase-shift symmetry of flows, with the difference that this phase independence follows the non-resonance conditions of equation (32) and will appear in terms indicated as $\mathcal{O}(\rho_j^4)$ in equations (33) and (34). These higher order terms can be neglected however for small ρ, and the radial dynamics can be solved separately for the phase evolution. If

$$\alpha_1(0) \neq 0$$

at criticality, equation (33) describes a pitchfork bifurcation at $\mu = 0$. Only the positive bifurcating branch is relevant,

$$\rho_H = \left[-\frac{\alpha}{\alpha_1}\right]^{1/2} \quad,$$

70

which, in combination with equation (34) describes a circle of radius ρ_H invariant after iteration of the dynamics. (In other words the branch can be said to be mapped into itself).

The bifurcation branch can be either supercritical or subcritical, depending on the sign of the ratio α/α_1, where

$$sgn\left[-\frac{\alpha}{\alpha_1}\right] = sgn\left[\frac{\mu}{\alpha_1(0)}\frac{d\alpha(0)}{d\mu} + \mathcal{O}(\mu^2)\right] = sgn\left[\mu\alpha_1(0)\right] \quad,$$

near μ. The invariant circle is therefore found when $\mu > 0$, if $\alpha_1(0) < 0$ (in the stable, supercritical case), while the branch is bifurcating in the case $\alpha_1(0) > 0$, when $\mu < 0$. The latter case is found to be unstable and subcritical.

V. CONCLUSION

In general one can assume dynamical processes to be defined by first order systems of the form (17), which depend on the parameter μ and describe motion in an n-dimensional phase space. The aim of bifurcation theory is to detect and analyse new branches of solutions as μ varies near the equilibrium point (μ_0, x_0), where $V(\mu_0, x_0) = 0$. In case x_0 is a hyperbolic equilibrium, the implicit function theorem guarantees that hyperbolicity remains, unless the eigenvalues of the stability matrix DV shift so as to touch the imaginary axis. When this happens, a bifurcation occurs.

The analysis described in the previous sections determines the existence of the new bifurcating solutions, their dynamics, as well as their stability. For μ sufficiently close to μ_0, the solutions fall within the neighbourhood of local attractivity for the centre manifold. Accepting, without loss of generality, that all continuously bifurcating branches of solutions lie in the invariant manifold, the dynamical system can be restricted to an independent dynamical system of dimension n_c, where n_c is the dimension of the centre subspace E^c. In particular, the resulting dynamical system describes all local bifurcations in the centre manifold.

In case of a hyperbolic equilibrium, the Hartman-Grobman theorem locally defines a topological conjugacy between the linear and the non-linear flow so that any qualitative change, or bifurcation, in the local linear dynamics, must be reflected in the non-linear dynamics as well. Applying near-identity coordinate changes to the reduced dynamical system, the resulting normal form can be easily analysed and the bifurcating solutions can be analytically worked out.

In the one-dimensional cases of saddle-node, transcritical and pitchfork bifurcations, both for flows and maps, as well as the two-dimensional cases of Hopf bifurcation, the above technique (see also section IId) proved to adequately provide an analysis of the bifurcating solutions in the neighbourhood of (μ_0, x_0), as well as information about their stability. In the case of period-doubling bifurcation, even though the analysis is carried out for the twice-iterated map, the two-cycle bifurcating branch is successfully calculated when the same technique is being implemented.

References

[1] M. Ablowitz and H. Segur, *Solitons and the inverse scattering transform*, SIAM, Philadelphia 1981

[2] V. Arnold, *Lectures on bifurcation in versal families*, Russ. Math. Surveys 27, 54, 1972

[3] V. Arnold, *Geometrical Methods in the theory of ordinary differential equations*, second edition, Springer, New York

[4] R. Bullough and P. Caudrey, *Solitons and the Korteweg-de Vries equation: integrable systems in 1834-1995*, Acta Appl. Math. 39 (1-3), 193-228, 1995.

[5] R. Burden, D. Faires, Numerical analysis, Prindle, Weber & Schmidt, Boston

[6] J. Crawford, *Introduction to bifurcation theory*, Reviews of modern physics, vol. 63, no. 4, 1991

[7] I. Cristie, D. Griffiths, A. Mitchell and J. Sanz-Serna, *Product approximation for non-linear problems in the finite element method*, IMA Journal of Numerical Analysis, 1, 253-266, 1981

[8] M. Delfour, M. Fortin and G. Payre, *Finite difference solution of a non-linear Schroedinger equation*, J. Comp. Phys., 44, 277-288, 1981.

[9] P. Drazin and R. Johnson, *Solitons : an introduction*, Cambridge University Press, N. Y. , 1988

[10] A. Fokas and I. Gelfand, *Integrability of linear and non-linear evolution equations and the associated non-linear Fourier transforms*, Letters in Mathematical Phys., 32, 189-210, 1994.

[11] A. Fokas and A. Its, *The linearisation of the initial-boundary value problem of the non-linear Schroedinger equation*, Clarkson University, INS no. 214, 1993.

[12] A. Fokas and V. Zakharov (eds), *Important developments in soliton theory*, Springer-Verlag, New York, 1993.

[13] G. Golub and C. Van Loan, *Matrix Computations*, The John's Hopkins University Press, Baltimore, Maryland

[14] D. Griffiths, A. Mitchell and J. Morris, *A Numerical Study of the NLS*, Report NA/52, University of Dundee, 1982.

[15] D. Griffiths, A. Mitchell and J. Morris, *A Numerical Study of the non-linear Schroedinger equation*, Comp. Methods in Appl. mech. and Eng., 45, 177-215, 1984.

[16] C. Grosch and S. Orszag, *Numerical solution of problems in unbounded regions : coordinate transforms*, J. Comp. Physics, 25, 273-296, 1977.

[17] J. Guckenheimer and P. Holmes, *Non-linear Oscillations, dynamical systems, and bifurcations of vector fields*, Applied mathematical sciences, 42, Springer, New York

[18] R. Hardin and F. Tappert, *Applications of the split-step Fourier method to the numerical solution of non-linear and variable coefficient wave equations*, SIAM Rev., Chronicle 15, 423, 1973.

[19] B. Herbst, A. Mitchell and J. Morris, *Numerical Experience with the non-linear Schroedinger equation*, Report NA/73, University of Dundee, 1983.

[20] B. Herbst, J. Morris and A. Mitchell, *Numerical Experience with the NLS*, J. Comp. Physics, 60, 282-305, 1985.

[21] D. Korteweg and G. de Vries, Phil. Mag. 39, 422, 1895.

[22] R. Kosloff and D. Kosloff, *Absorbing Boundaries for Wave Propagation Problems*, Journal of Computational Physics 63, 363-376, 1986.

[23] B. Lake, H. Yuen, H. Rungaldier and W. Ferguson, *Non-linear deep-water waves; theory and experiment. Part 2. Evolution of a continuous wave train*, J. Fluid Mech., 83, 49-74, 1974.

[24] L. Landau and E. Lifshitz, Quantum Mechanics, Pergamon, Oxford, 1965.

[25] A. Mitchell and J. Morris, *A self adaptive finite difference scheme for the non-linear Schroedinger equation*, Arab Gulf Journal of Scientific Research, 1, 461-472, 1981.

[26] J. Sans-Serna, *An explicit finite difference scheme with exact conservation properties*, J. Comp. Phys., 52, 273-289, 1982.

[27] J. Sans-Serna and V. Manoranjian, *A method for the integration in time of certain partial differential equations*, J. Comp. Phys., 52, 273-289, 1982.

[28] J. Sans-Serna, *Methods for the numerical solution of the non-linear Schroedinger equation*, Mathematics of Computation, 43, 21-27, 1984.

[29] J. Scott Russel, *Report on waves*, Rept. 14th meeting of the British Association for the advancement of science, John Murray, London, 1844, 311-390 + 57 plates

[30] Y. Tourigny and J. Morris *An Investigation into the Effect of Product Approximation in the Numerical Solution of the Cubic NLS*, J. Comp. Phys., 76, 103-130, 1988.

[31] J. Weidmeman and B. Herbst *Split-step methods for the solution of the non-linear Schroedinger equation*, SIAM J. Numer. Anal., v. 23, 485-506, 1986.

[32] G. Whitam, *Linear and non-linear waves*, John Wiley, New York, 1974.

[33] V. Zakharov and D. Shabat, *Exact theory of two-dimensional self-focusing and one-dimensional self-modulation of waves in non-linear media*, Soviet Physics JETP, 34, 62-69, 1972.

[34] N. Zabusky and M. Kruskal, *Interaction of solitons in a collisionless plasma and the recurrence of initial states*, Phys. Rev. Letters 15, 240, 1965.